Regolith Stratigraphy and Gold Distribution within Tributary Palaeochannels near Gindalbie and Kurnalpi, Kalgoorlie Region, Western Australia

By

Stephen F Lynn, Bach App Sc (App Geol)

Submitted in fulfilment of the requirements for the degree of

Master of Economic Geology

University of Tasmania, December 1994

This Thesis contains no material which has been accepted for a degree or diploma by the University of Tasmania or any other institution, except by way of background information and duly acknowledged in the Thesis, and to the best of the Candidate's knowledge and belief no material previously published or written by another person except where due acknowledgement is made in the text of the Thesis.

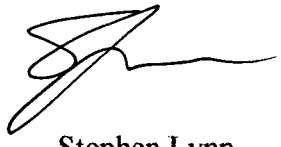

Stephen Lynn

12 December 1994

This Thesis is not to be made available for loan or copying for six months following the date this statement was signed. Following that time this Thesis may be made available for loan and limited copying in accordance with the *Copyright Act 1968*

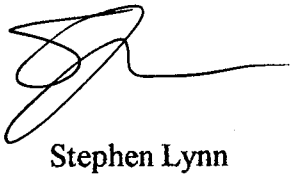

Stephen Lynn

10 April 1995

ABSTRACT

This study investigates two sites within the Roe Palaeodrainage system in the Kalgoorlie Region of Western Australia. Both are located over southward draining tributary palaeochannels that have incised into already deeply weathered Archaean lithologies. The pre-palaeochannel regolith is only partly preserved at Gindalbie due to the site's proximity to the main trunk palaeoriver. However at Kurnalpi, there is extensive preservation of the pre-existing laterite profile beneath the palaeochannel sediments and permits an estimation of the maximum depth of palaeochannel incision: That is 25-30 metres at Kurnalpi; 40-50 metres at Gindalbie; 60-70 metres in the trunk channel.

The palaeochannel sediments comprise a basal sand facies that is generally confined to the palaeoriver bed, and a conformable upper clay facies that blankets the entire palaeodrainage valley. The sediments have also been lateritized, resulting in an extensive ferruginization of the upper profile (Fe-induration, Fe-nodules and pisoliths, and mega-mottles), and at least at Gindalbie, a prominent redox front at 18-20 metres depth below which reducing conditions prevail. The sand facies has been palynologically dated by others as Middle to Late Eocene in age, thus constraining the lateritization events to pre and post-Eocene.

At Kurnalpi, colluvial/alluvial incision has extensively truncated the upper profile of both the transported and in-situ regolith. This event has occurred after post-Eocene lateritization and appears to be confined to the mid and upper slopes of the catchment area.

At both sites gold mineralization is extensive but is confined to the environs of the palaeochannels.

At Gindalbie gold is almost exclusively distributed as discrete horizontal horizons within the palaeochannel sediments below the main redox front, with the highest grades located directly above the palaeochannel thalweg. No bedrock mineralization was encountered; and gold distribution appears to be controlled by groundwater regimes/chemistry and host lithology mineralogy.

At Kurnalpi Archaean lode-style gold mineralization is spatially associated with supergene gold within both the palaeochannel sediments and the in-situ regolith. The highest gold grades from both regolith profiles are distributed about a vertical plane through the channel thalweg, with placer gold located at the base of the palaeochannel sand facies. All gold mineralization appears to be derived initially from basement lodes and distribution patterns reflect local controls such as bedrock structure, basement lithology, channel morphology and groundwater movement.

Acknowledgements

The author gratefully acknowledges the permission and support of Mt Kersey Mining N.L. management, in particular Mr Ed Eshuys, to complete this Thesis and Master of Economic Geology Degree.

Dr Charles Butt offered advice on general content and supergene gold morphology and chemistry.

Mr Phil Bock at RMIT performed the SEM analyses and photomicrographs.

Mr Bob Crosley sectioned the spherical pisoliths.

Analabs in Perth performed the ICPMS analyses on the spherical pisoliths.

Australian Assay Laboratories in Kalgoorlie performed the fire assay Au analyses on the drill samples.

Ann Stewart prepared the base plan for the Kurnalpi drillhole locations.

TABLE OF CONTENTS

1.0 INTRODUCTION

1.1 Objectives and background

This thesis is an investigation of the regolith landform relationships and gold distribution patterns within two study areas located on north-south oriented tributary palaeochannels of the Roe Palaeodrainage system in the Kalgoorlie region of Western Australia. The Roe palaeodrainage is an eastward draining inactive river system of Mesozoic to Late Eocene age(Kern & Commander 1993, Smyth & Button 1989), that has become choked with sediment and today is characterized by a series of shallow ephemeral salt lakes.

The study areas are located near Gindalbie and Kurnalpi, approximately 30 km NE and 70 km ENE of Kalgoorlie respectively. The sites examine a 3 -5 kilometre length along separate tributary palaeochannels both of which drain to the south into the Yindarlgooda North trunk palaeoriver of the Roe palaeodrainage system (Fig. 1.1).

Both sites were investigated by the author for Mt Kersey Mining N.L. from 1992 to 1994 as part of a regional exploration program testing for gold mineralisation associated with tributary palaeochannels in the Eastern Goldfields Region of Western Australia. The basis of this exploration effort was a model developed from similar mineralization at the Lady Bountiful Extended (LBE) gold mine, approximately 50 kilometres north of Kalgoorlie

LBE is host to at least three hundred thousand ounces of economic gold, the majority of which (having been mined) is contained within the base of a tributary palaeochannel on the northern margin of the Roe palaeodrainage. Gindalbie, Kurnalpi and LBE all occupy similar geomorphological locations; draining from the

margin of the palaeodrainage catchment into the Yindarlgooda trunk palaeoriver. Gindalbie and Kurnalpi are located 30 km and 80 km respectively downstream along the Yindarlgooda branch from LBE (Fig. 1.1)

At LBE there is a close spatial association of bedrock lode-style mineralisation and gold concentration in the palaeochannel. It is unclear as to what extent placer and/or chemical remobilization processes have contributed to economic gold concentration and this question is open to further investigation, though is not part of this study.

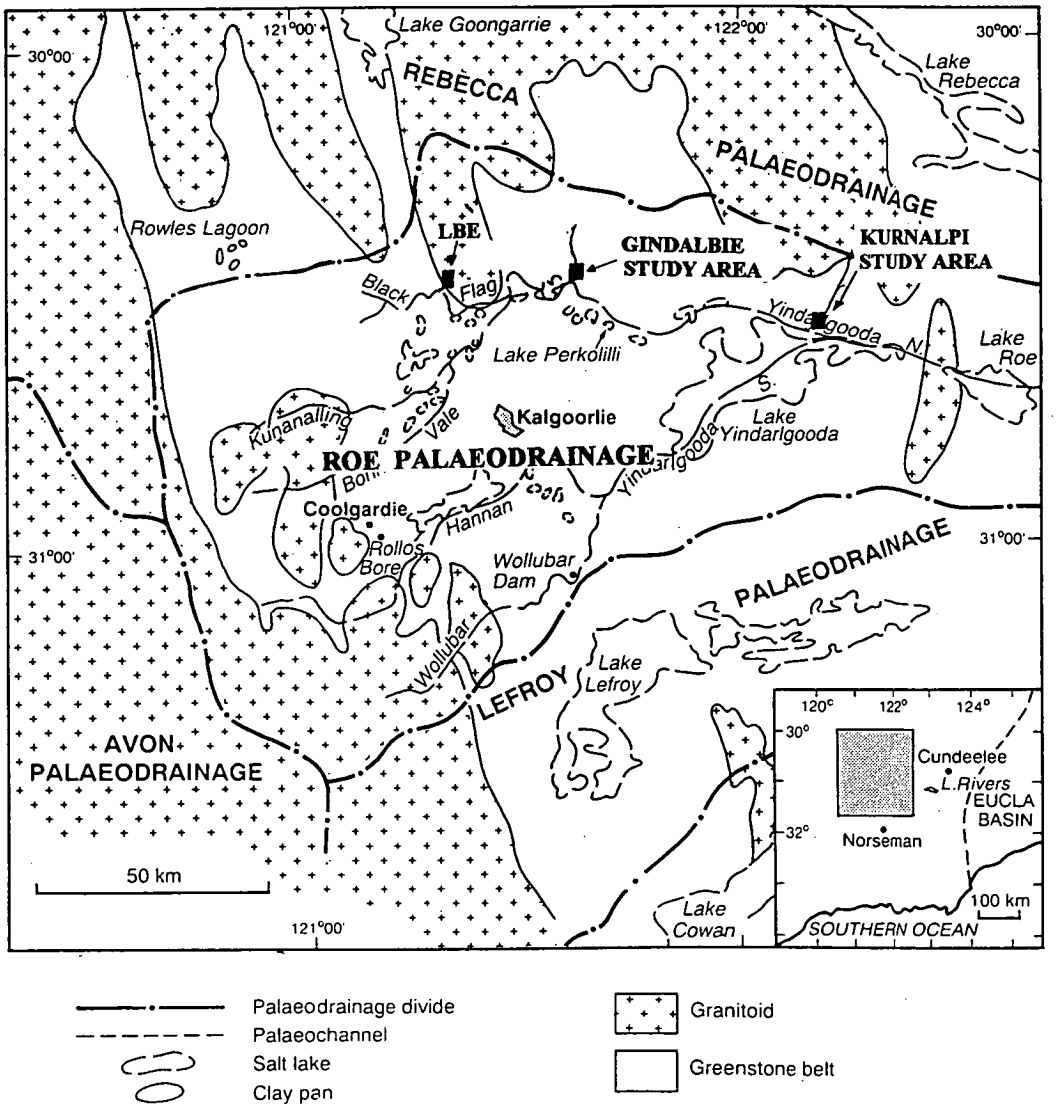

Figure 1.1 Location map of the study areas within the Roe palaeodrainage (modified after Kern & Commander, 1993)

1.2 Methods

The gold exploration by Mt Kersey Mining N.L. in both study areas included extensive Reverse Circulation (RC) drilling programs. In both cases the drilling data provides a comprehensive assessment of the regolith profile across and along the strike of the palaeochannel valleys. Hence this study is based solely on drillhole data and field observations.

The RC drilling method provided relatively reliable and accurate samples under difficult drilling conditions when palaeochannel sediments were encountered. Unconsolidated colluvial gravels, swelling puggy clay and wet unconsolidated sand are the ubiquitous components of the transported regolith.

In some instances, unreliable gold assays were encountered due to contamination from previous wet or high grade samples. In such cases suspect assays have not been included in the gold distribution analysis for this study. For example; at Kurnalpi, bottom hole anomalism was seen to boost gold assays in the first few metres in the following drillhole from background levels of 20 ppb up to 50 - 100 ppb (redrilling, but not in the original sequence, produced no anomalism) (Lintern, 1994).

All holes at both sites have been drilled vertically to blade refusal. This effectively means that the drillholes have penetrated through the regolith to the saprock/bedrock boundary of the underlying basement rocks. The drillholes have been sampled by riffle splitting into generally 4 (but occasionally 2) metre composites. The samples were analysed for Au via 50 gram fire assay at Australian Assay Laboratories in Kalgoorlie.

2.0 REGIONAL SETTING

2.1 Geology

The Eastern Goldfields Province of the Yilgarn Craton of West Australia is characterized by north to north-west trending Archaean greenstone assemblages comprising mafic, ultramafic and felsic volcanic suites interleaved with volcanic and non-volcanic derived sediments, and subsequently intruded by granitoid plutons (Swager et al., 1990).

The Kalgoorlie region has been subdivided into a number of tectono-stratigraphic greenstone assemblages of similar rock suites and common deformation histories, of which the Kalgoorlie Terrane and the Kurnalpi Terrane are relevant to this study. Both the Gindalbie and Kurnalpi study areas are located within the Kurnalpi Terrane, but are contained within separate fault bounded lithostratigraghic domains. LBE is located within the Kalgoorlie Terrane. (Swager et al. 1990, Swager 1994).

2.2 Regolith

The Eastern Goldfields Province, as has the rest of the Yilgarn Craton, been subject to extensive deep weathering since at least the Mesozoic (Ollier et al. 1988, Clarke 1994b). The resultant laterite profile varies over different lithologies but is characterized by kaolinization due to leaching of alkali elements and ferruginization of the upper profile especially over more mafic lithologies (Anand & Smith 1993).

In the Kalgoorlie region the laterite profile has been extensively truncated on upland areas and is seemingly poorly developed and truncated on mid to lower slopes - with widespread development of acid red soils (Anand & Smith 1993).

In the Kalgoorlie region the laterite profile has been extensively truncated on upland areas and is seemingly poorly developed and truncated on mid to lower slopes - with widespread development of acid red soils (Anand & Smith 1993).

Within lowland areas (which comprise somewhere around 50% of the land surface) the dominant landforms are sediments of the Roe Palaeodrainage system and colluvial debris usually resting on deep saprolite.

The Roe Palaeodrainage was initially reconstructed from aerial photographs showing an extensive series of interconnected salt lakes draining over several hundred kilometres towards the Great Australian Bight (van de Graaff et al. 1977) The lakes are the present day expression of palaeochannel valleys that have become choked with sediment.

There is an apparent southward migration of the active channel within the east-west oriented valleys since sediment infill began; - caused by regional southward tilting of approximately 1.5 minutes about the Jarrahwood Axis (van de Graaff et al. 1977, Smyth & Button 1989) (Fig. 2.1)

Further evidence of relative uplift since initiation of palaeochannel incision is provided by:-

i) A regional decrease in maximum erosional depth within individual palaeodrainage catchments from north to south (Smyth & Button 1989).

ii) Drainage reversal of the Cowan Palaeodrainage from north and east to southward draining (Clarke 1994a)

iii) Surface drainage and groundwater flow reversal to the south on the catchment divide of the Roe Palaeodrainage; in the Wollubar area (Kern & Commander 1993); and in the Rowles Lagoon - Mt Carnage area, where a

north-east draining palaeochannel in the Rebecca Palaeodrainage has surface drainage diverting to the southern Roe catchment.

iv) The elevation of sediments deposited during Middle to Late Eocene marine transgression by 110 to 150 metres (Clarke 1994a) (Fig. 2.1)

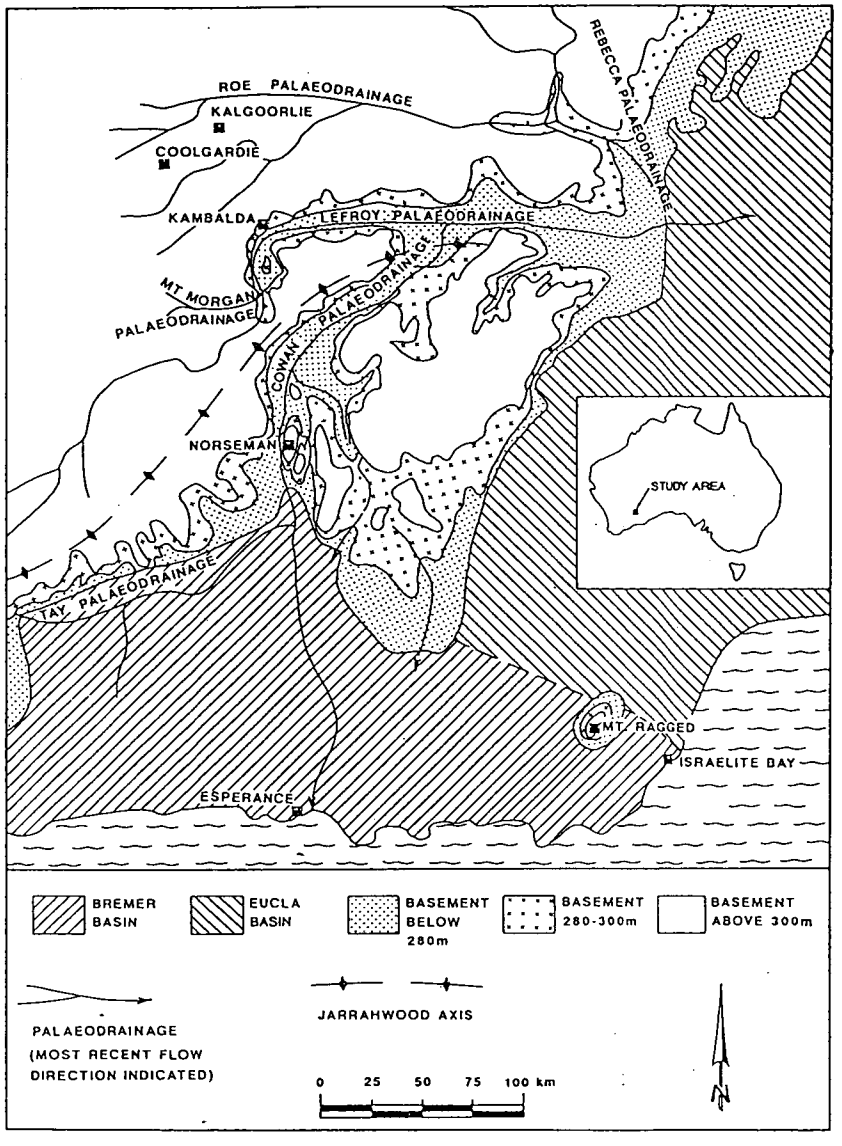

Figure 2.1 Location of marine basins east of the Roe Palaeodrainage. Marine transgression below 300m and below 280m (from Clarke 1994a)

3.0 GINDALBIE

3.1 Introduction

The Gindalbie study area is centred on the lower reaches of a north-south oriented tributary palaeochannel of the Yindarlgooda (Roe) palaeoriver. The investigation site is adjacent to the confluence of the tributary and main trunk palaeoriver and extends north some 4½ kilometres along the tributary channel. It is approximately 2 kilometres due south of the 14 Mile Dam and some 15 km NNE of Kanowna. Location maps are presented as Fig. 2.1 & 3.1.

Investigation of the Gindalbie study area is based on a total of 204 reverse circulation drillholes located along 10 east-west traverses. The holes were generally drilled at 40 metre spacings along each traverse, and the traverses were in turn spaced at 500 metres intervals (Fig. 3.2). Drillhole numbers are prefixed by the letters "KSC" and were completed in two separate programs. Hole numbers in the KSC400-500 series range were completed first along east-west traverses. Holes in the KSC2000 series range were completed after a local grid had been established using the fence that bisects the study site as a base line. The fence line is about 5° off magnetic north so the two series of traverses are not quite parallel. For the purposes of the site investigation though, this problem was immaterial as the drill traverses were sited to intersect the tributary palaeochannel perpendicular to the channel axis. Good coverage from bank to bank has been achieved which provides for an accurate three dimensional picture of the channel morphology.

At the confluence site the tributary channel occupies a valley approximately 600 metres wide and 50-60 metres deep. The trunk palaeoriver is substantially larger. Groundwater investigation bores nearby indicate that the trunk drainage

valley is some 1500 metres wide and 60-70 metres deep (Commander et al., 1991). Both palaeochannel valleys are filled with a sedimentary sequence comprising basal fluvial sand and overlying laminated lacustrine clay. The sand occupies the deepest portions of the channel and extends generally to about half the width.

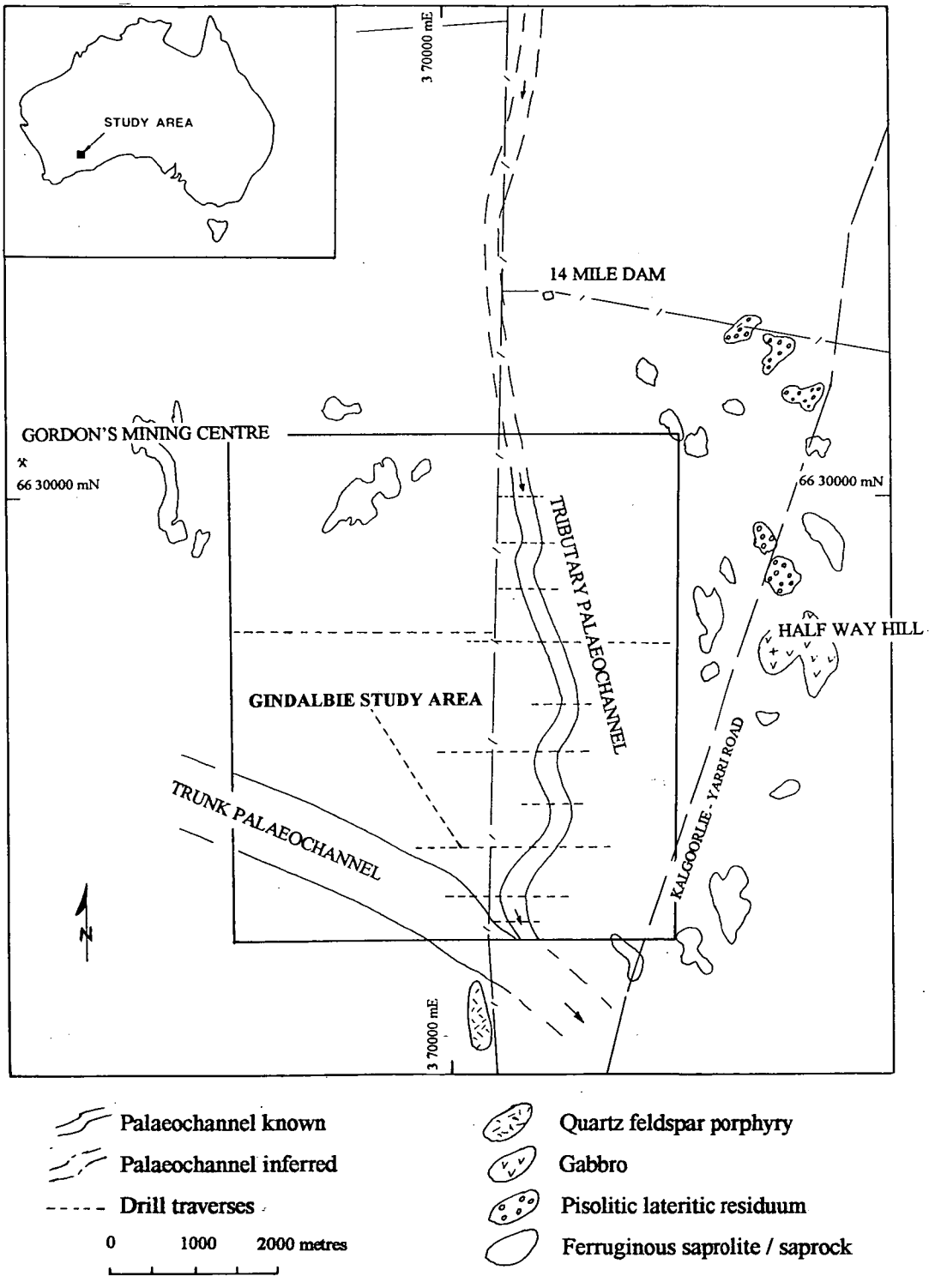

Figure 3.1 Location of Gindalbie study area

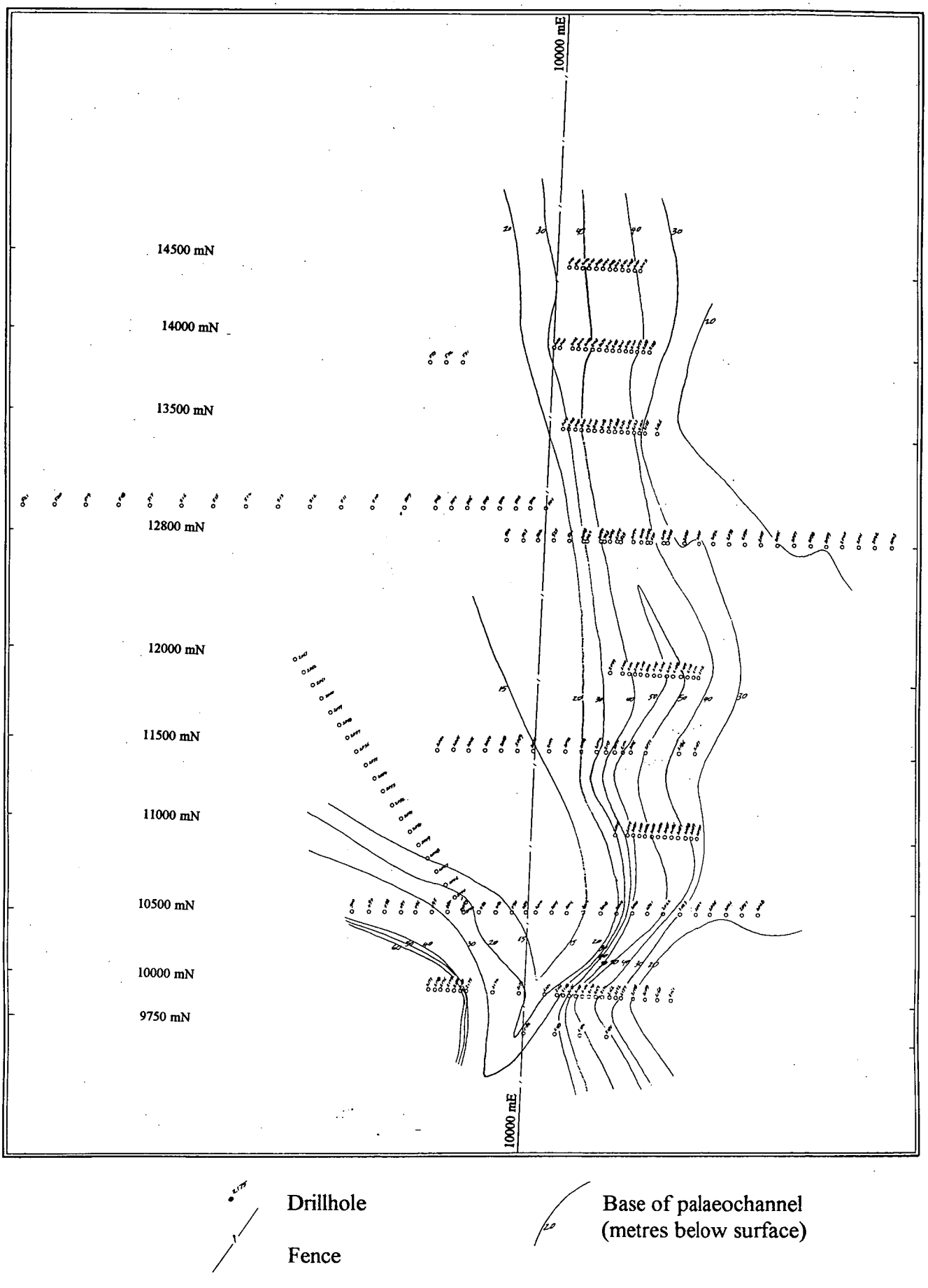

Figure 3.2 Depth to base of palaeochannel contours, drillhole locations and orientation of local grid at the Gindalbie study area

The Roe palaeodrainage at the study site has incised into a deeply weathered Archaean felsic basement, consisting of predominantly quartz-feldspar porphyry and felsic volcaniclastic rocks, but including mafic dykes and volcanics. The action of the palaeodrainage has stripped the basement to varying degrees, depending on the channel morphology and distance from the main trunk palaeoriver. But all of the pre-existing surface over which the palaeochannel flowed has not been spared at least some incision.

3.2 Regolith stratigraphy

3.2.1 Overview

The regolith at the Gindalbie site can be divided into 3 time-constrained units based on correlating the sand facies here to that of the Middle to Late Eocene sand in the Roe palaeoriver (Kern & Commander, 1993; Smyth & Button, 1989). The divisions from surface to basement are as follows:

1. Modern colluvium.
2. Eocene palaeochannel sediments comprising an upper clay facies and basal sand facies.
3. Pre Eocene lateritized Archaean basement.

3.2.2 Recent colluvium

This unit blankets the entire study area and ranges in thickness from 2 to 6 metres but noticeably thins towards outcropping basement (Fig 3.4).

It is composed of red-brown colluvial clays, with occasional ironstone pisoliths, ferruginous granules and rarer lith fragments. Pedogenic carbonate is well developed in the top two or three metres of the colluvium across the entire study area, imparting a distinct pink-brown colour (Fig. 3.5A). Where the colluvium cover is thin, carbonate induration is developed throughout the unit, but is inhibited by the underlying Fe-indurated lacustrine clay. Carbonate concentration is generally highest over the first one or two metres then gradually decreases with depth. It also varies sporadically across the Gindalbie site but is within the range of 5 to 14 wt % Ca (Lintern, 1994).

The colluvium unconformably overlies lacustrine clays of presumable Eocene age. The contact between the two units is essentially horizontal but bows-up slightly approaching outcropping lateritized basement.

3.2.3 Lacustrine clay

This unit is correlatable to the Perkolilli Shale of Kern & Commander (1993) and conformably overlies the sand facies of the palaeochannel. Outside the confines of the channel proper it unconformably overlies Archaean basement.

The palaeochannel sand facies is confined to the incised channel proper on both the tributary channel and the main Yindarlgooda palaeoriver. The clay facies is much more widespread in its distribution. Its conformable lower and unconformable upper margins are basically horizontal, thus its thickness is very much dependent on the channel morphology. It completely mantles the saddle of Archaean basement between the two palaeorivers close to the junction in the south, and in the study area is only constrained on the east.

The clay varies in thickness from approximately 30 metres over the deepest parts of the palaeochannel and gradually pinches-out on the margins (some 1500 metres to the east on line 12800N ; to the west and south-west its distribution is not constrained by drilling , but would most likely extend some 2 or 3 km).

The unit is composed of laminated uniform fine clays of an apparent lacustrine origin (Kern & Commander, 1993; Smyth & Button, 1989); no evidence is observed of marine deposition. The clays have been heavily modified with a lateritization overprint, resulting in abundant Fe concentration and induration above a prominent redox front at about 18-20 metres downhole depth (Fig. 3.5). The clays can be subdivided about the main redox front into 2 components:

(a) An upper red-brown coloured oxidised zone with abundant Fe concentration/induration;

(b) A lower dark grey reduced clay zone with much less Fe and minor internal redox fronts.

This division is useful in determining the relative timing of lateritization events, the depth of channel incision, and the controls on gold mineralization. (section 3.3 deals with the lateritization overprint in more detail)

3.2.4 Fluvial sand

The sand facies of the palaeochannel is correlated to the Wollubar Sandstone of Kern & Commander (1993) which has been palynologically dated by the same authors as late Middle to early Late Eocene age. Smyth & Button (1989) also report a Late Eocene to Early Oligocene age for the sand facies of the main trunk palaeochannels in the Roe palaeodrainage.

The sand unit is confined to the channel proper where incision into basement is most pronounced. In the tributary palaeochannel it has a maximum thickness of approximately 15 metres and a width of some 300 metres; in the main truck drain it is double these dimensions.

The sand is clean, poorly sorted, and predominantly of quartz composition. It is very angular with only an occasional well-rounded grain being observed, and has a distinct fining-upwards gradation with a coarse basal gravel a metre or so thick.

The top of the sand grades to a kaolinite clay rich facies that sits as a lens 2 to 3 metres thick between the sand and the lacustrine clay. The facies gradation to kaolinite clay rich - sand poor is also evident on the channel flanks (Figs. 3.3 & 3.4). There is no visual evidence of carbonaceous matter or manganese concretions (except for elevated Mn from one pisolith sample; see section 3.), both of which have been reported from the trunk palaeoriver (Kern & Commander, 1993; Smyth & Button, 1989).

3.2.5 Archaean saprolite

The Archaean basement consists of deeply weathered quartz-felspar porphyry, felsic volcaniclastics, carbonaceous shales, mudstones and mafic intrusives.

Saprolite development is ubiquitous and varies according to rock type but generally is in the order of 20-40 metres. The depth of weathering beneath the centre of the channel is roughly the same as that on the flanks (Figs. 3.3 & 3.4); implying either minimal incision by the channel or subsequent weathering after incision. The latter scenario is favoured based on evidence suggesting two separate lateritization events (below).

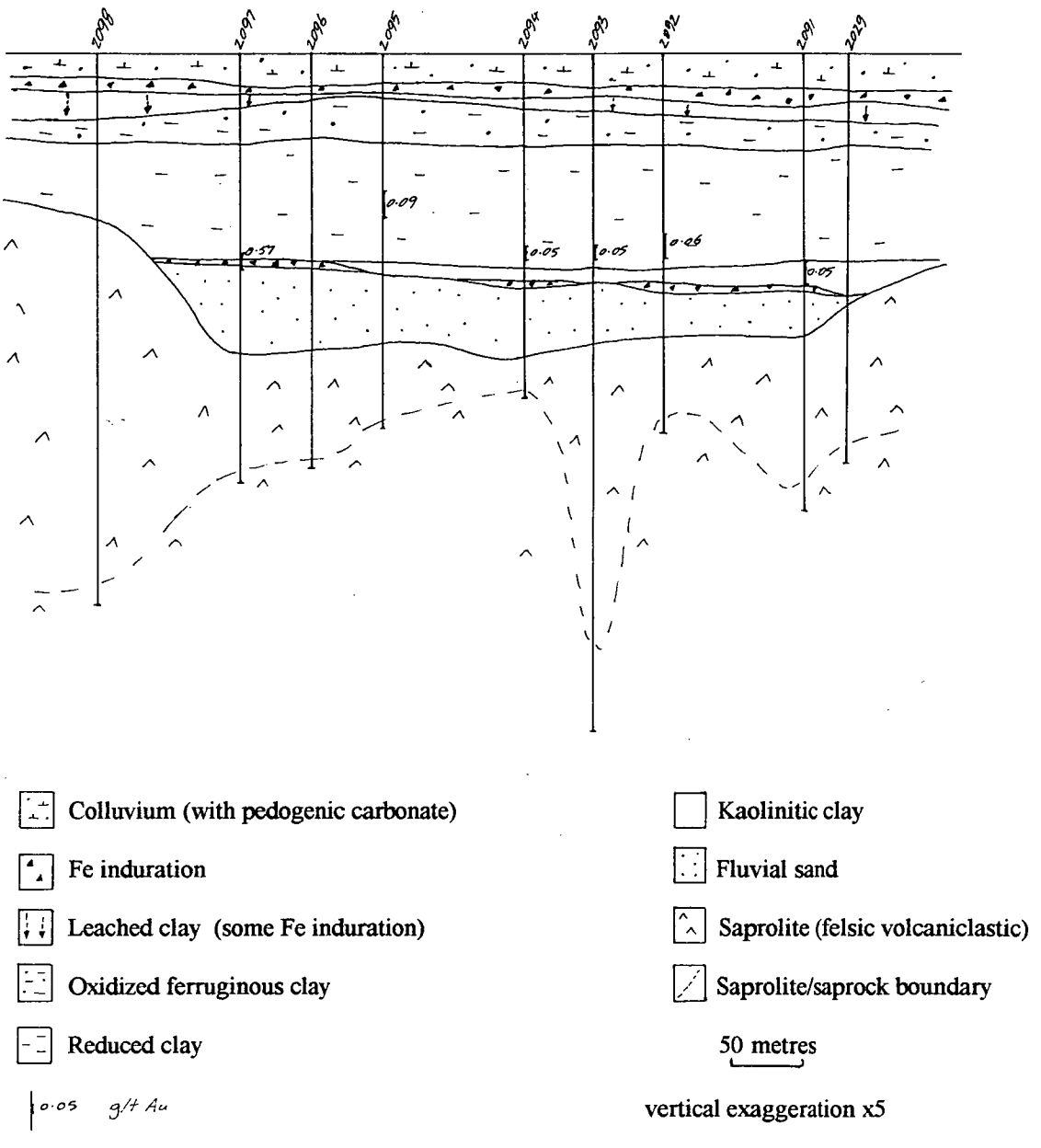

Figure 3.3 Cross section across palaeochannel on line 12800 mN

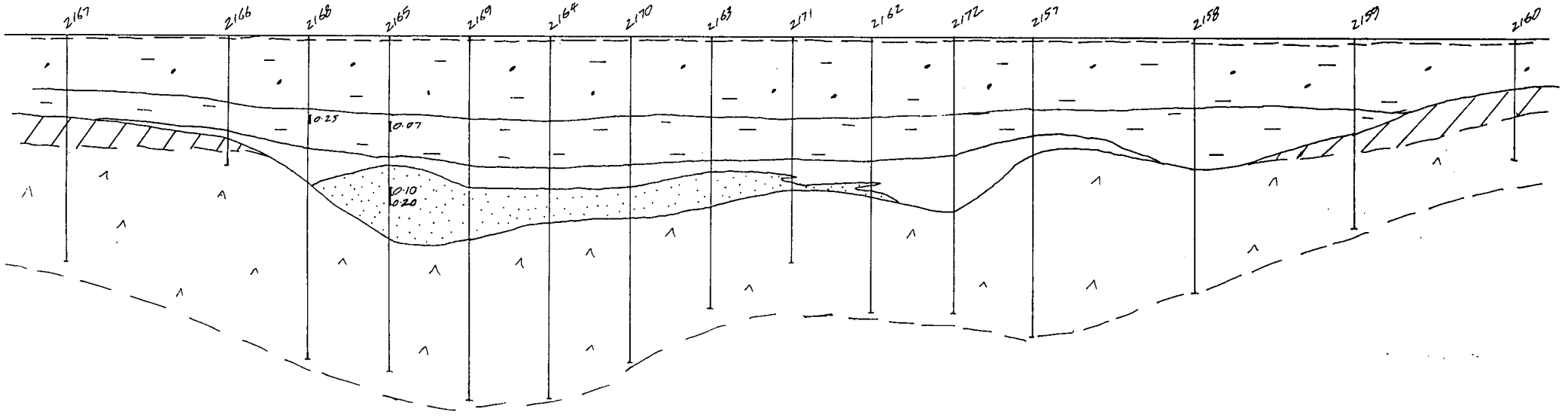

TRANSPORTED REGOLITH

- Pedogenic carbonate within colluvium
- Oxidized lacustrine clay
- Reduced lacustrine clay
- Kaolinitic clay/sand
- Fluvial sand

IN-SITU REGOLITH

- Ferruginous saprolite
- Leached saprolite
- Saprock/bedrock interface

0.20 g/t Au

50 metres

vertical exaggeration x 5

Figure 3.4 Cross section along the 10000 mN line; tributary channel

The location of the Gindalbie site at the confluence of the tributary and trunk palaeorivers has at least partly controlled the depth of incision of the channels relative to the preserved laterite profile within the saprolite. Pisolitic and nodular lateritic residuum, the upper-most units of many complete Yilgarn laterite profiles (Anand & Smith, 1993; Smith & Anand, 1990; Butt, 1988), are exposed in outcrop some 1.5 kilometres to the east of the study area. In the vicinity of the channels at Gindalbie the upper laterite profile has been completely stripped away. The cross-sectional information (Figs 3.3 & 3.4) indicates that the tributary channel has incised through at least 40 metres of basement; the main channel probably 50 metres. In fact, the pre-channel landsurface height probably equates to the present surface at Gindalbie, though is probably shaped as a broad valley.

High on the channel banks, and on the saddle between the two palaeochannel valleys, the basal unit of the upper ferruginous laterite profile is preserved; this mainly consists of nodular Fe-indurated saprolite. As the palaeochannel cuts deeper the lower portions of the laterite profile are progressively exposed and preserved beneath the channel (red-brown to yellow ferruginous saprolite with occasional ironstone concretions). This process culminates at and adjacent to the channel thalweg where all ferruginous components of the laterite profile are completely stripped away and an intensely leached saprolite remains.

Leached (bleached) saprolite clays grade to fresh bedrock after about 40 metres depth. The majority of the underlying bedrock is quartz-rich felsics and weathers on compositional and colour criteria in a similar way to that of the sand - sand/clay facies of the palaeochannel, thus making visual differentiation difficult.

3.3 Post-Eocene lateritization

3.3.1 Overview

As stated previously, lateritization of the palaeochannel sediments is well developed and consistent over the Gindalbie site. The post-Eocene laterite profile is best observed over the deepest parts of the channel where the clay and sand facies are thickest. The upper ferruginous component of the profile is partially truncated by the rising basement on the eastern channel margin and both channel flanks in the north; thus obscuring individual lateritization events.

A type section depicting both the post and pre Eocene lateritization events is presented as Figure 3.5. The generalized post-Eocene laterite profile has been subdivided into a number of zone which are persistent and may be correlated throughout the study area; they are summarized below:

(i) An upper zone of iron enrichment approximately 2-3 metres thick. Abundant angular Fe nodules forming a partial duricrust within red brown ferruginous clays.(Fe over 50% by volume)

(ii) A zone of leaching usually extending 2-3 metres; clays are bleached, angular Fe nodules are abundant to common (generally <.50% Fe by vol.).

(iii) A second zone of ferruginous clays ± Fe nodules extending 3-4 metres.

(iv) A mottled clay zone extending 4-5 metres; equivalent to the so called mega-mottles seen at QED (Kanowna)(R. Anand pers. comm. 1993) and LBE.

(v) A zone of ferruginous clays, commonly containing rounded Fe nodules, extending 4-5 metres; terminating at a redox front with the reduced clays, invariably at about 18-20 metres downhole depth.

(vi) This main redox boundary is distinguished by a distinct colour change from red-brown above to grey/dark - grey below, and is also the site of extremely abundant spherical Fe-pisolith development. The pisoliths are concentrated at the redox front where they may account for up to 50% of the volume of the sediment and extend below into the reduced clays some 5 to 10 metres at a greatly reduced concentration. Distinguished from other Fe-pisoliths by almost perfect sphericity and multiple concentric rinds.

(vii) Reduced clays; - quite uniform, apart from occasional spherical pisoliths they contain much less Fe products than the upper profile. Frequent minor internal redox fronts and associated colour changes

(viii) Bleached kaolinitic clay / sandy clay / sand; often with a band of Fe induration at the base of the sandy clay or kaolinitic clay facies (Fig. 3.3), but otherwise a complete absence of Fe-concentration.

3.3.2 Spherical pisoliths

The pisoliths are almost perfectly spherical and are composed of concentric goethite - kaolinite rinds accreted on mainly fossil plant material, though a lesser percentage have other Fe concretions and pisoliths at their core (Fig 3.6 C,D&E).

The pisoliths have formed in situ. Their perfectly preserved nature and growth within the well laminated reduced clays is shown in Fig. 3.6 B. They develop due to ferrolysis at the redox front and the accumulations seen here are likely to be the result of substantial stillstands in the water table (Lawrance 1993). There is evidence that the pisoliths may have developed during multiple separate accretion phases. Figure 3.6 E is a photo micrograph of an individual pisolith with an inner core of goethitic rinds over an elongate plant fossil. This inner pisolith has

TYPE-SECTION

PRE AND POST EOCENE LATERITE PROFILES

KSC 2168 10240 mE 10000 mN

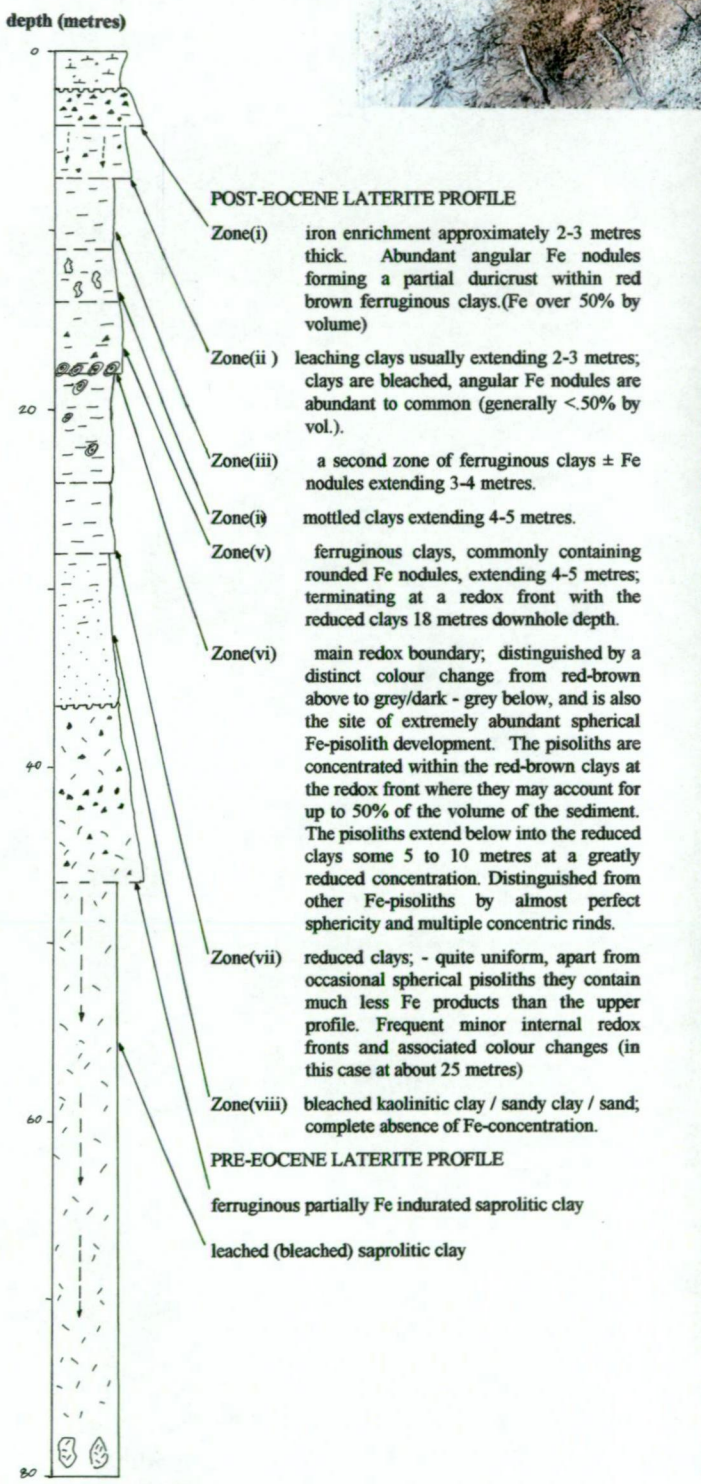

POST-EOCENE LATERITE PROFILE

Zone(i) iron enrichment approximately 2-3 metres thick. Abundant angular Fe nodules forming a partial duricrust within red brown ferruginous clays.(Fe over 50% by volume)

Zone(ii) leaching clays usually extending 2-3 metres; clays are bleached, angular Fe nodules are abundant to common (generally <.50% by vol.).

Zone(iii) a second zone of ferruginous clays ± Fe nodules extending 3-4 metres.

Zone(iv) mottled clays extending 4-5 metres.

Zone(v) ferruginous clays, commonly containing rounded Fe nodules, extending 4-5 metres; terminating at a redox front with the reduced clays 18 metres downhole depth.

Zone(vi) main redox boundary; distinguished by a distinct colour change from red-brown above to grey/dark - grey below, and is also the site of extremely abundant spherical Fe-pisolith development. The pisoliths are concentrated within the red-brown clays at the redox front where they may account for up to 50% of the volume of the sediment. The pisoliths extend below into the reduced clays some 5 to 10 metres at a greatly reduced concentration. Distinguished from other Fe-pisoliths by almost perfect sphericity and multiple concentric rinds.

Zone(vii) reduced clays; - quite uniform, apart from occasional spherical pisoliths they contain much less Fe products than the upper profile. Frequent minor internal redox fronts and associated colour changes (in this case at about 25 metres)

Zone(viii) bleached kaolinitic clay / sandy clay / sand; complete absence of Fe-concentration.

PRE-EOCENE LATERITE PROFILE

ferruginous partially Fe indurated saprolitic clay

leached (bleached) saprolitic clay

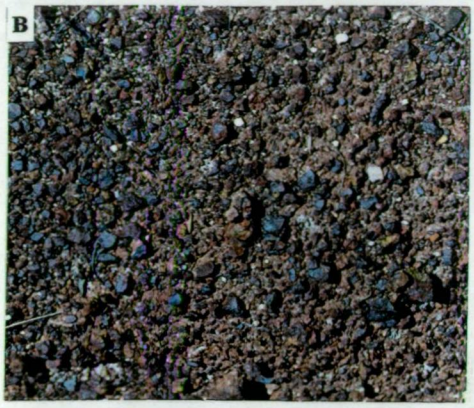

Figure 3.5 Type section of the pre and post Eocene laterite profile based on hole KSC 2168 - southern section of the tributary palaeochannel.

A) drillspoil of hole KSC 2168; - piles represent individual metres laid out in rows of 10; - start of hole in bottom right hand corner. B) Fe induration at 4 metres depth. C) main redox front; - pisolith development within the red-brown clays. D) Fe induration within the upper saprolite.

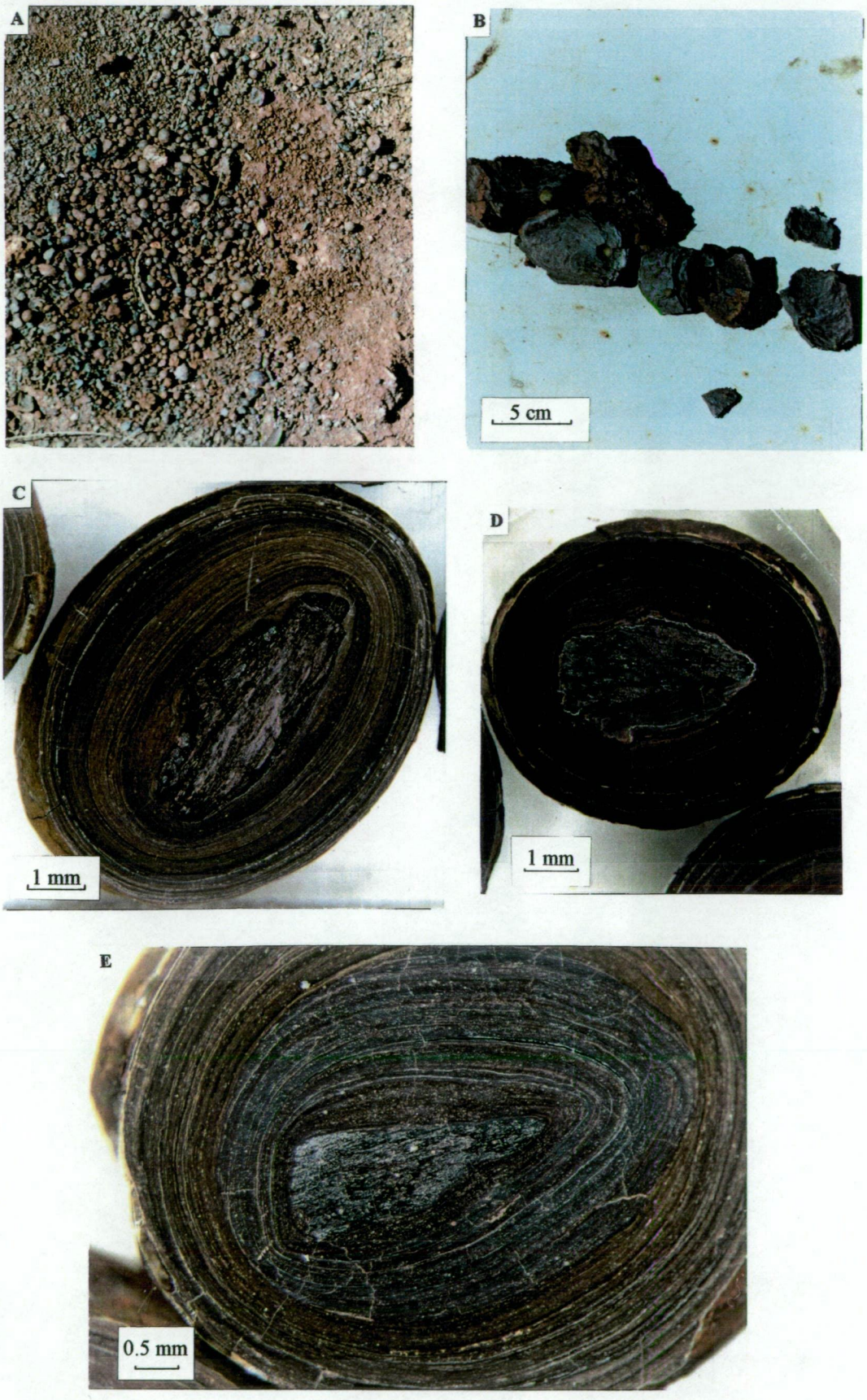

Figure 3.6 Spherical pisoliths developed in the lacustrine clay facies of the palaeochannel A) extremely abundant pisolith development at the main redox front. B) pisoliths developed in-situ in laminated clay. C),D)&E) fossil plant material at the pisolith core.

subsequently undergone further accretion at some latter time. This is indicated by the lighter coloured goethitic layers that comprise the outer half of the pisolith, which have a different geometry to those of the inner core.

Pisolith distribution is mostly confined to the tributary channel at the Gindalbie site. They are ubiquitous along the length of the channel within a zone whose western boundary is approximately directly above the channel thalweg and extend to the east beyond the sand facies margin by 200 - 300 metres. They are virtually totally absent along the western flank of the tributary and within the main trunk palaeochannel even though the redox front at which the main accumulation occurs is continuous over these areas.

22 pisolith samples from a range of holes along the tributary channel were collected for trace element analysis (Table 3.4). The sample were analysed for a range of gold pathfinder elements, with a view to determine whether there existed any correlation between pisolith geochemistry and gold anomalism within the palaeochannel sediments. The pisolith elemental concentration should be read in conjunction with the gold distribution patterns and for that reason is discussed in section 3.4.4.

3.4 Gold mineralization

3.4.1 Overview

All gold mineralisation at Gindalbie is confined to the environs of the palaeochannels (Fig. 3.7). Gold is distributed as discreet semi-horizontal horizons within the palaeochannel sediments, occasionally at the basal unconformity, and as a few minor sporadic instances within saprolite directly beneath the channel.

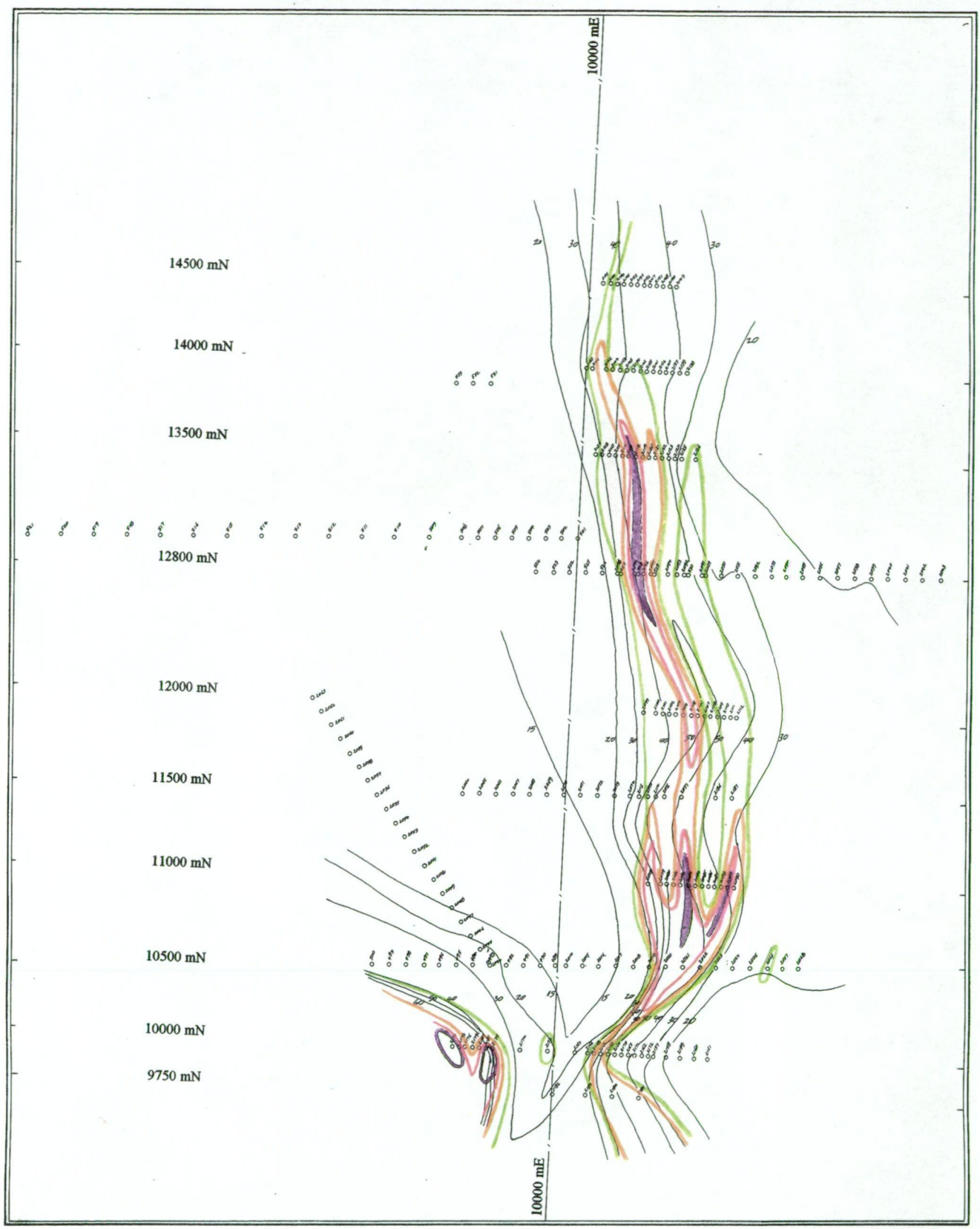

Figure 3.7 Gold distribution within the regolith at Gindalbie (Au content determined as grams per tonne x metres)

The majority of the drillholes in the study area are located along the tributary channel thus a reliable understanding of the gold distribution within this system is possible. On the other hand, only one drill line has partially traversed the main palaeoriver (Fig. 3.2). Gold is present here in significant quantities at distinct lithological/geochemical boundaries with important implications for transportation and precipitation mechanisms, but broad distribution patterns across and along the main palaeochannel valley cannot be determined in this study.

The two sections (Figs. 3.3 & 3.4) display typical gold distribution patterns within the regolith, including within both the sediments of the palaeodrainage system and the Archaean basement. Appendix 1. is a table of all anomalous gold recorded in drill intercepts at Gindalbie.

The best gold grades in the tributary channel are typically from 26 to 34 metres depth; ranging from 2 metres @ 0.5 g/t to 2 metres @ 1.0 g/t. The best gold grade in the trunk channel is 2m @ 1.82 g/t from 60 metres. None of these grades are economic under current extractive and economic conditions.

3.4.2 Gold mineralization within the tributary palaeochannel

Within the tributary channel the majority of the gold is located at the base of the clay unit immediately above the sand - sandy clay facies (Table 3.1). Less frequently gold also occurs above and below this boundary within the reduced clay and sand units respectively. A very minor amount of gold is present at the base of the channel sands and at the saprolite - saprock boundary.

Anomalous trends in the tributary channel are very much controlled by the channel morphology. Even though the majority of the gold mineralization is not located at the base of the channel but above it, the highest gold values on each

section correspond to the position of the channel thalweg, then tend to taper either side (Fig. 3.7). Once free of the confines of the channel proper, and in this study that is defined as the section that contains the sand facies, gold mineralization drops back to background levels (which is below the fire assay detection limit used here; < 0.01 ppm). Gold concentration within the basement saprolite is also almost universally at background levels. Only five drillholes have intersected minor anomalous gold within this horizon, three of which are beneath the deepest portion of the channel.

DRILLHOLE NO.	CO-ORDINATES	ANOMALOUS Au INTERSECTIONS	LITHOLOGICAL CONTROL ON MINERALIZATION
KSC 2155	10120E 14500N	2m @ 0.13 g/t from 30m	base of clay/top of sand interface
KSC 2132	10120E 14000N	2m @ 0.21 g/t from 32m	base of clay/top of sand interface
KSC 2142	10320E 14000N	4m @ 0.04 g/t from 28m	base of clay/top of sand interface
KSC 2127	10160E 13500N	2m @ 0.06 g/t from 32m	base of clay/top of sand interface
KSC 2115	10200E 13500N	4m @ 0.06 g/t from 28m	base of clay/top of sand interface
KSC 2118	10320E 13500N	4m @ 0.25 g/t from 28m	base of clay/top of sand interface
KSC 2119	10360E 13500N	4m @ 0.04 g/t from 28m	base of clay/top of sand interface
KSC 2120	10400E 13500N	6m @ 0.11 g/t from 26m	base of clay/top of sand interface
KSC 2097	10350E 12800N	2m @ 0.57 g/t from 28m	lacustrine clay/sandy clay interface
KSC 2094	10550E 12800N	2m @ 0.05 g/t from 28m	base of clay/top of sand interface
KSC 2093	10600E 12800N	4m @ 0.04 g/t from 28m	base of clay/top of sand interface
KSC 2092	10650E 12800N	4m @ 0.06 g/t from 26m	base of clay/top of sand interface
KSC 2091	10750E 12800N	4m @ 0.04 g/t from 30m	base of clay/top of sand interface
KSC 2100	10520E 12000N	2m @ 0.07 g/t from 32m	lacustrine clay/sandy clay interface
KSC 2101	10560E 12000N	2m @ 0.06 g/t from 30m	lacustrine clay/sandy clay interface
KSC 2102	10600E 12000N	4m @ 0.04 g/t from 28m	lacustrine clay/sandy clay interface
KSC 2104	10680E 12000N	4m @ 0.06 g/t from 30m	lacustrine clay/sandy clay interface
KSC 2105	10720E 12000N	6m @ 0.11 g/t from 32m	lacustrine clay/sandy clay interface
KSC 2106	10760E 12000N	4m @ 0.12 g/t from 30m	base of clay/top of sand interface
KSC 2107	10800E 12000N	6m @ 0.09 g/t from 28m	base of clay/top of sand interface
KSC 2110	10920E 12000N	2m @ 0.08 g/t from 32m	base of clay/top of sand interface
KSC 2076	10600E 11500N	2m @ 0.19 g/t from 30m	base of clay/top of sand interface
KSC 2077	10700E 11500N	2m @ 0.12 g/t from 32m	base of clay/top of sand interface
KSC 2083	10760E 11000N	2m @ 1.00 g/t from 32m	base of clay/top of sand interface
KSC 2084	10800E 11000N	4m @ 0.11 g/t from 24m	within reduced lacustrine clay unit
KSC 2088	10960E 11000N	2m @ 0.05 g/t from 32m	base of clay/top of sand interface
KSC 2089	11000E 11000N	2m @ 0.50 g/t from 28m	lacustrine clay/sandy clay interface
KSC 2020	10650E 10500N	2m @ 0.38 g/t from 28m	base of clay/top of sand interface
KSC 2021	10750E 10500N	2m @ 0.35 g/t from 32m	base of clay/top of sand interface
KSC 2184	10360E 9750N	2m @ 0.07 g/t from 26m	base of clay/top of sand interface

Table 3.1 Anomalous gold at the facies interface between the sand/sandy clay and the lacustrine clay within the tributary palaeochannel.

3.4.3 Gold mineralization in the trunk palaeochannel

Gold distribution within the main trunk palaeochannel follows distinctly different patterns to that of the tributary channel. The main mineralisation trends occur as 2 discreet horizontal horizons; one within the reduced lacustrine clay, the other at the base of the sand facies, both of which also occur in the tributary channel (the latter being very uncommon in the tributary channel). Both trends also display good continuity from hole to hole along the drill section (Fig. 3.8).

Very weak anomalous gold is also present within the lower portion of the oxidized lacustrine clay (zone v. of the post-Eocene lateritization). Gold within this horizon is completely absent in the tributary channel. No anomalous gold is contained however within the weathered bedrock profile beneath the trunk palaeochannel (Fig. 3.8).

Of the two main gold trends, the upper horizon is contained within the reduced component of the lacustrine clay unit (zone vii), a few metres below the main redox boundary. Gold values are typically low but consistent across the section (Fig 3.8). This location in the regolith as a site for gold accumulation is common to both channels but appears to be more widespread in the trunk palaeoriver. Table 3.2 (below) lists anomalous gold at this horizon.

DRILLHOLE NO.	CO-ORDINATES	ANOMALOUS Au INTERSECTIONS	LITHOLOGICAL CONTROL ON MINERALIZATION
KSC 2177	9400E 10000N	6m @ 0.21 g/t from 26m	top of reduced clay
KSC 2178	9440E 10000N	6m @ 0.17 g/t from 26m	top of reduced clay
KSC 2176	9480E 10000N	4m @ 0.13 g/t from 28m	within reduced lacustrine clay unit
KSC 2179	9520E 10000N	2m @ 0.10 g/t from 30m	within reduced lacustrine clay unit
KSC 2180	9560E 10000N	4m @ 0.14 g/t from 28m	within reduced lacustrine clay unit
KSC 2181	9600E 10000N	4m @ 0.09 g/t from 28m	within reduced lacustrine clay unit
KSC 2175	9640E 10000N	4m @ 0.16 g/t from 28m	base of channel clay (no sand unit)

Table 3.2 Anomalous gold within the reduced clays of the trunk palaeoriver

The second significant gold horizon within the main channel is along the unconformity at the base of the sand unit. Relatively high gold values are concentrated in one hole (2m @ 1.82 g/t Au in hole KSC 2181: see Table 3.3), then progressively diminish to low levels laterally away from this location. But again, as with the gold bearing reduced clay above, there is a persistence of mineralization along this interface (Fig. 3.8).

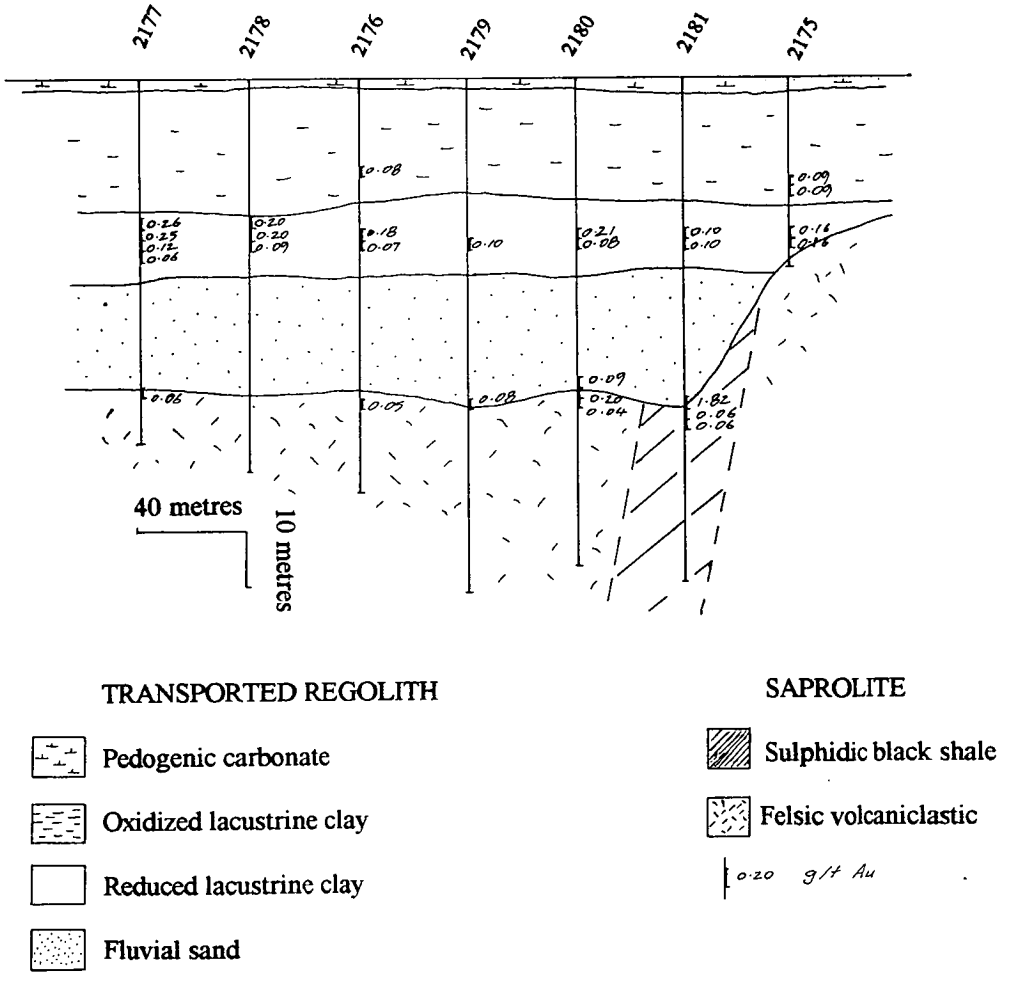

Figure 3.8 Cross section of the trunk palaeochannel on line 10000 mN

DRILLHOLE NO.	CO-ORDINATES		ANOMALOUS Au INTERSECTIONS	LITHOLOGICAL CONTROL ON MINERALIZATION
KSC 2177	9400E	10000N	2m @ 0.07 g/t from 58m	sand/saprolite unconformity
KSC 2176	9480E	10000N	2m @ 0.05 g/t from 60m	sand/saprolite unconformity
KSC 2179	9520E	10000N	2m @ 0.08 g/t from 60m	sand/saprolite unconformity
KSC 2180	9560E	10000N	4m @ 0.15 g/t from 56m	sand/saprolite unconformity
KSC 2181	9600E	10000N	2m @ 1.82 g/t from 60m	sand/saprolite unconformity
KSC 2175	9640E	10000N	4m @ 0.16 g/t from 28m	base of channel clay (no sand unit)

Table 3.3 Anomalous gold at the trunk palaeochannel/saprolite unconformity

In drillhole KSC 2181 the palaeochannel is in direct contact with a weathered pyritic carbonaceous shale (estimated 30% pyrite content by vol.). The sulphide has suffered only minor oxidation; fresh pyrite being ubiquitous at the unconformity through the regolith to fresh bedrock some 30 metres below. Adjacent drillholes have intersected felsic volcaniclastic and possibly minor mafic/ultramafic intrusive lithologies. KSC 2181 is the only hole where the juxtaposition of the palaeochannel and sulphidic black shales is observed and clearly the mineralogy of the bedrock is controlling gold deposition.

3.4.4 Trace element analysis of spherical pisoliths

22 pisolith samples from the main redox front and the underlying lacustrine clays of the tributary channel were analysed for a suite of chalcophile elements (Table 3.4). The aim was to determine whether or not any correlation existed between the pisolith geochemistry and the gold distribution in the palaeochannel sediments.

Two element suites were determined. The first, a range of gold pathfinder elements is common to all samples (Au As Mo Sn Sb Ag Pt Pd Pb W Bi), whilst the second (Cu Zn Be Mn Nb U) only applies to approximately half the samples; - this was done purely as a cost saving measure.

The gold pathfinder suite of elements chosen for analysis is typical of that found as anomalous concentrations in the upper laterite profile over many Yilgarn gold deposits (Davy & El-Ansary, 1986; Smith et al., 1989; Smith & Anand, 1990). These gold pathfinder elements have generally been remobilized from the primary ore horizon (Archaean mafic associated lode-style) and as such are unique to the environs of the primary source (subject to dispersion). It is probable, based on the distribution patterns, host lithologies, lack of bedrock anomalism, etc, that the gold within the palaeochannel sediments at Gindalbie is secondary in origin (and probably far removed from source) and is therefor unlikely to be associated with an elevated pathfinder suite.(The trace element composition of the pisoliths were determined prior to the completion of the drilling at Gindalbie and it was unclear at that stage as to the origin of the gold. cf. Kurnalpi)

The pisoliths were mostly collected from the main redox front within the lacustrine clays. As previously stated, pisolith development here is ubiquitous, though all gold mineralization is distributed in the sediments below this horizon. 3 samples were collected from the reduced clay below the main redox front where pisolith development is much reduced and tends to be sporadic.

The sampled drillholes were distributed along selected traverses down the length of the tributary channel. A range of samples were collected from drillholes with anomalous gold and some from barren drillholes (Table 3.4). Of the 3 samples from lower in the profile, two were from barren holes, and one (SL210) was collected from a mineralized horizon. This was in fact the only sample collected from within an anomalous gold horizon.

Of the 19 samples from the main redox front, none display any elemental (including Au) correlation with underlying gold both across the profile and along

the channel thalweg. Sample SL210, collected from an horizon grading 0.48 g/t Au over 4 metres within the reduced clays about 10 metres below the main redox front, displays a different elemental distribution than that of the other samples:

Of the gold pathfinder suite, Au alone is slightly elevated (at 4.97 ppb about double the response in the other samples), the other elements are within the general range for all the samples. Of the relatively more mobile second suite, almost all are elevated, especially Mn which appears to be 6-7 times that of other samples. A relatively high manganese oxide content within the reduced clay may be enhancing or controlling gold enrichment in this environment. Manganese oxide is a known scavenger of mobile ions including Au; manganese/cobalt/gold mineralization has been reported from palaeochannel sediments at Kanowna, just a few kilometres south of the Gindalbie site on the other side of the trunk palaeoriver (Wilson, 1984; Mann & Webster, 1990).

SAMPLE NO.	Au	As	Mo	Sn	Sb	Ag	Pt	Pd	Pb	W	Bi	Cu	Zn	Be	Mn	Nb	U	HOLE\DEPTH (m)	Anomalous Au in d'hole g/m (depth)
SL200	2.85	44	5.27	1.20	2.88	0.26	0.67	< 0.50	25.1	1.02	0.21	n/a	n/a	n/a	n/a	n/a	n/a	KSC2164\26-27	nil
SL201	2.15	74	8.08	0.88	5.71	0.10	1.50	0.77	51.0	0.80	0.37	n/a	n/a	n/a	n/a	n/a	n/a	KSC2163\18-20	nil
SL202	2.20	45	5.09	0.66	2.73	0.12	0.95	< 0.50	29.5	0.57	0.14	n/a	n/a	n/a	n/a	n/a	n/a	KSC2163\27-29	nil
SL203	2.69	70	9.53	0.80	5.94	0.16	1.48	0.80	52.5	0.93	0.49	n/a	n/a	n/a	n/a	n/a	n/a	KSC2171\19-20	nil
SL205	2.71	190	10.10	0.84	5.44	0.12	1.49	1.41	64.8	1.77	0.49	46.3	31.4	0.86	96.4	4.81	4.60	KSC2099\18-20	0.20 (22-26)
SL206	2.13	210	8.34	0.73	9.89	0.13	2.23	1.48	62.3	0.93	0.77	33.5	18.5	0.81	94.6	3.93	4.46	KSC2100\18-20	0.14 32-34
SL208	1.92	160	12.00	0.94	4.60	0.24	1.50	1.72	65.1	1.47	0.49	148.0	23.3	0.84	107.0	4.51	4.85	KSC2104\19-21	0.24 30-34
SL209	2.36	130	8.49	0.93	4.08	0.14	1.52	1.30	41.5	1.10	0.52	63.2	46.9	0.62	201.0	3.96	3.43	KSC2106\20-21	0.48 30-34
SL210	4.97	100	11.30	0.96	2.14	0.26	1.73	1.05	53.4	1.06	0.49	152.0	218.0	2.93	746.0	5.77	9.87	KSC2106\31-33	0.48 30-34
SL211	2.03	150	10.60	0.89	5.85	0.18	1.60	1.16	56.8	1.88	0.64	51.4	22.9	0.77	148.0	4.64	3.96	KSC2108\20-22	nil
SL212	3.06	140	10.50	0.95	4.36	0.15	2.18	1.03	54.7	1.27	0.68	37.1	12.6	0.71	82.9	3.42	3.49	KSC2110\20-22	0.16 32-34
SL213	2.94	66	5.45	2.65	5.98	0.17	1.83	0.88	32.9	0.92	0.32	n/a	n/a	n/a	n/a	n/a	n/a	KSC2112\21-22	0.36 42-44
SL214	1.63	75	6.61	1.22	5.54	0.16	2.08	1.00	36.0	1.44	0.56	n/a	n/a	n/a	n/a	n/a	n/a	KSC2155\18-19	0.26 30-32
SL215	1.90	230	7.98	0.96	7.42	0.10	2.28	1.11	38.1	1.12	0.60	n/a	n/a	n/a	n/a	n/a	n/a	KSC2146\17-19	nil
SL216	1.52	180	8.81	2.44	7.69	0.16	2.03	0.99	41.1	1.18	0.62	n/a	n/a	n/a	n/a	n/a	n/a	KSC2148\19-20	nil
SL217	1.24	70	8.81	0.91	7.06	0.10	1.82	0.95	39.8	1.07	0.50	n/a	n/a	n/a	n/a	n/a	n/a	KSC2149\19-20	nil
SL218	1.90	150	13.1	1.11	7.15	0.12	1.63	1.42	53.9	0.98	0.47	n/a	n/a	n/a	n/a	n/a	n/a	10200E 9550N\20+	unknown
SL219	1.81	140	8.89	0.78	6.46	< 0.10	1.24	1.20	55.6	0.65	0.42	n/a	n/a	n/a	n/a	n/a	n/a	10400E 9550N\20+	unknown
SL220	2.95	140	10.20	0.86	4.48	0.16	1.68	1.22	66.3	1.03	0.41	42.6	24.8	0.87	108.0	4.02	4.68	KSC2082\20-22	0.82 40-42
SL221	1.81	150	9.76	1.58	5.16	0.16	0.95	0.84	75.8	0.84	0.41	37.2	19.8	0.91	80.6	3.83	5.32	KSC2083\22-24	2.00 32-34
SL222	2.52	140	8.40	0.93	3.92	< 0.10	1.42	1.13	57.1	0.88	0.36	42.7	18.7	0.62	77.4	3.80	3.37	KSC2089\20-22	1.00 28-30
SL223	2.16	170	9.68	1.08	6.01	0.19	1.60	1.12	78.7	1.10	0.59	49.0	27.9	0.81	126.0	4.46	8.49	KSC2097\18-20	1.14 28-30
UNITS	ppb	ppm	ppm	ppm	ppm	ppm	ppb	ppb	ppm	ppm	ppm	ppm	ppm	ppm	ppm	ppm	ppm		
Detection Limit	1.00	1	0.1	0.5	0.5	0.1	0.50	0.50	1.0	0.1	0.10	2.0	2.0	0.1	0.5	0.20	0.05		

n/a: not analysed

	Au	As	Mo	Sn	Sb	Ag	Pt	Pd	Pb	W	Bi	Cu	Zn	Be	Mn	Nb	U
Mean	2.338636	128.3636	8.954091	1.104545	5.476818	0.151818	1.609545	1.062727	51.45455	1.091364	0.479545	63.90909	42.25455	0.977273	169.8091	4.286364	5.138182
Standard E	0.164224	11.3503	0.442291	0.107859	0.384442	0.011022	0.088997	0.067629	3.091923	0.068244	0.031509	#N/A	#N/A	#N/A	#N/A	#N/A	#N/A
Median	2.155	140	8.85	0.935	5.625	0.155	1.6	1.08	53.65	1.045	0.49	46.3	23.3	0.81	107	4.02	4.6
Mode	1.9	140	8.81	0.93	#N/A	0.16	1.5	0.4	#N/A	0.93	0.49	#N/A	#N/A	0.81	#N/A	#N/A	#N/A
Standard D	0.770277	53.2376	2.074527	0.505905	1.803194	0.051698	0.417435	0.317208	14.5024	0.320094	0.147793	43.33745	58.96876	0.654784	194.4801	0.646564	2.117767
Variance	0.593327	2834.242	4.303663	0.25594	3.251508	0.002673	0.174252	0.100621	210.3197	0.10246	0.021843	1878.135	3477.315	0.428742	37822.52	0.418045	4.484936
Kurtosis	5.708192	-0.85952	0.009298	5.262889	0.549048	0.206105	0.109069	0.612708	-0.62139	1.125592	0.480859	1.689781	10.32881	10.37663	9.995987	1.744317	1.807628
Skewness	1.885802	-0.01702	-0.2381	2.384154	0.260856	0.772477	-0.38975	-0.29406	-0.00767	0.978899	-0.38202	1.774654	3.183376	3.183291	3.119947	1.135287	1.626474
Range	3.73	186	8.01	1.99	7.75	0.18	1.61	1.32	53.6	1.31	0.63	118.5	205.4	2.31	668.6	2.35	6.5
Minimum	1.24	44	5.09	0.66	2.14	0.08	0.67	0.4	25.1	0.57	0.14	33.5	12.6	0.62	77.4	3.42	3.37
Maximum	4.97	230	13.1	2.65	9.89	0.26	2.28	1.72	78.7	1.88	0.77	152	218	2.93	746	5.77	9.87
Sum	51.45	2824	196.99	24.3	120.49	3.34	35.41	23.38	1132	24.01	10.55	703	464.8	10.75	1867.9	47.15	56.52
Count	22	22	22	22	22	22	22	22	22	22	22	11	11	11	11	11	11

Table 3.4 Trace element analysis of spherical pisoliths from the tributery channel, Gindalbie.

4.0 KURNALPI

4.1 Introduction

The Kurnalpi study area is located approximately 3 kilometres west of the abandoned Kurnalpi town site and immediately south of the Kurnalpi - Kalgoorlie road. (Fig. 4.1)

At this site a tributary palaeochannel has incised into an intercalated Archaean sequence of basalt and komatiite. The channel also cuts across a major regional shear, the Avoca Shear, where bedrock lode style gold mineralisation and palaeochannel-hosted gold mineralisation are mutually developed.

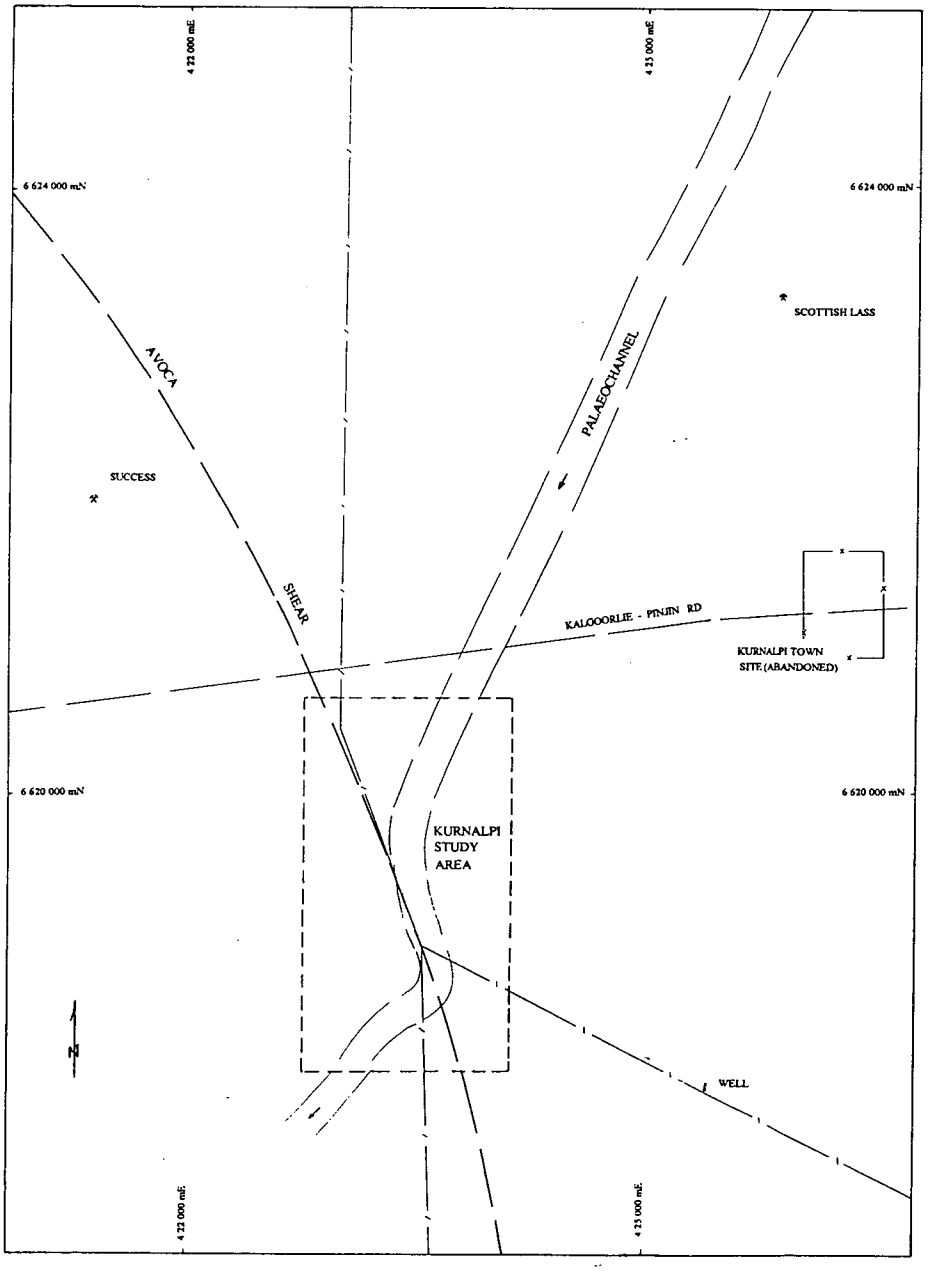

Figure 4.1 Location map

The Avoca Shear is a west-dipping boundary fault separating the Jubilee and Karonie-Yindi domains within the Kurnalpi Terrane. (Swager 1994) It is at least 80 km long trending NNW and extends several kilometres into the crust.

Both the Jubilee and Karonie-Yindi domains contain an interleaved sequence of mafic/ultramafic and felsic volcaniclastic and clastic rock units with intrusive granitoid emplacement to the north (Swager, 1994). Within the study area both domains are present in roughly equal portions. Both are dominated by intercalated basalt and komatiite units, with felsic lithologies completely absent from the Jubilee domain and present only as minor trachytic to trachyandesitic interflows in the Karonie-Yindi domain (Fig. 4.2).

Within the study area the location of the Avoca Shear has been inferred from aeromagnetic data and drill intercepts. The aeromagnetic data also suggests that the palaeochannel valley to the north-east may coincide with and be controlled by a secondary shear trending at a bearing of approximately 35°. On the other hand, drilling under the palaeochannel to the north-east has not indicated the presence of shearing within the bedrock or any obvious displacements, and the possibility exists that the observed magnetic trend may be due to contrast within the regolith caused by the palaeochannel sediments. In any case the palaeochannel does trend at 35° north-east of the study area with the head waters originating in a granite dominated terrain some 7 kilometres away (The source of the quartz sand within the channel).

The Avoca Shear has a dramatic influence on the morphology of the palaeochannel. As the channel approaches the shear from the north-east the valley steepens and narrows, the channel has a more pronounced meander, and alters its course by approximately 90° as it is captured by the shear. It then flows along the trace of the Avoca Shear some 800 metres before breaking-out and continuing on its

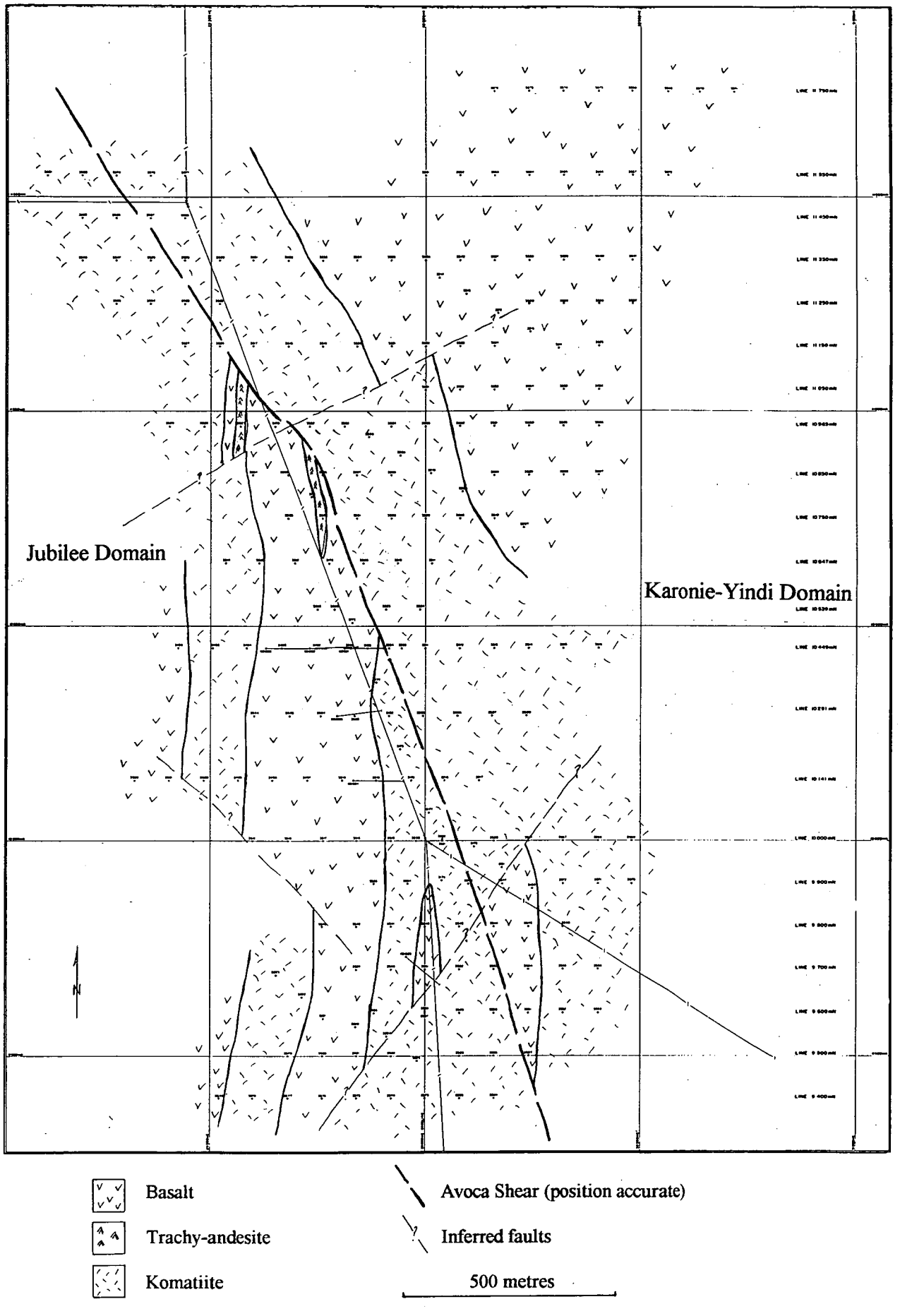

Figure 4.2 Simplified interpreted Archaean geology of the Kurnalpi study area.

original flow direction towards the main Yindarlgooda (Roe) palaeoriver approximately 4 kilometres to the south-west (Figs 4.1 & 4.3).

4.2 Regolith stratigraphy

4.2.1 Overview

The palaeochannel sediments are typical of those described at Gindalbie (this paper) and within the trunk palaeorivers by Kern & Commander (1993) and Smyth & Burton (1989). They comprise a lower sand facies confined to the channel proper and an upper clay facies that mantles and extends beyond the channel banks. Whereas the palaeochannel sediments at Gindalbie are difficult to differentiate from similarly composed and weathered Archaean regolith, those at Kurnalpi are distinctly incongruous juxtaposed against the mafic/ultramafic basement and present much less difficulty in determining the precise location of the unconformity. The relative thickness and width of the individual units within the channel profile is shown in the three cross-sections (Figs 4.6, 4.7, 4.8).

The Archaean rocks are deeply weathered both beneath the channel and on the flanks, with an extensive laterite profile being substantially preserved especially on the sides and periphery of the channel.

The palaeochannel sediments are in turn overlain by a relatively thick sequence of lateritic detritus dominated colluvial/alluvial clays. This unit is clearly not contemporaneous with the palaeochannel sediments having incised its own valley in to the lacustrine clays and mantling the Archaean regolith on the channel flanks.

The regolith stratigraphy can be again divided into three time-constrained units based on correlating the sand facies of this palaeochannel to that of the trunk

palaeoriver, which is dated at Middle to Late Eocene in age (Kern & Commander, 1993 and Smyth & Burton, 1989). Thus:

1. Post-Eocene colluvium.
2. Eocene palaeochannel sediments comprising a lower quartz sand facies and upper lacustrine clay facies.
3. Pre-Eocene lateritization of Archaean basement.

4.2.2 Post-Eocene colluvium/alluvium

Colluvial/alluvial sediments blanket the majority of the study area and have a basal unconformity with both the lacustrine clay facies of the palaeochannel sediments and with the Archaean rocks. They are thickest over the deepest portions of the underlying palaeochannel and tend to pinch-out to the north-west and south-east where Archaean basement crops out. The three cross-sections (Figs. 4.6, 4.7, 4.8) and the relative-height contour map of the unconformity (Fig. 4.4) provide a guide to distribution and thickness of the colluvium across the Kurnalpi site.

The sediments are essentially composed of a clay and polymict lateritic gravel with minor accessory sand. A rudimentary fining-upward gradation is observed over most of the area. Clay is the dominant component in the upper profile, then fairly rapidly grades to gravel dominated at about 4 or 5 metres depth.

The gravel is composed of a polymict mixture containing abundant rounded to sub-rounded ferruginous granules, angular to sub-rounded ferruginous saprolite, and lateritic pisoliths - usually with well developed cutans (Figs. 4.9A & 4.10C). The relative proportions of these components changes with depth. The ferruginous

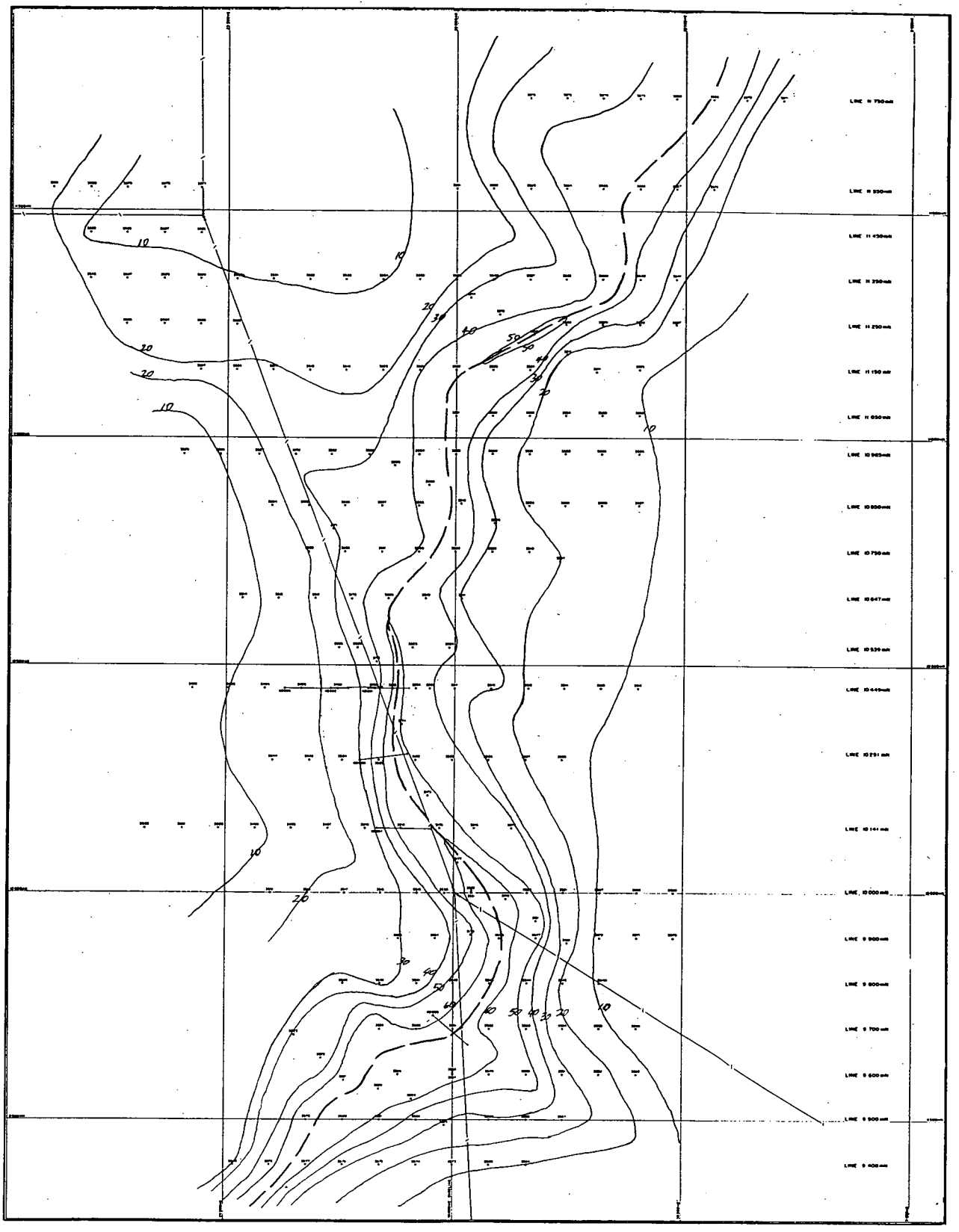

Figure 4.3 Contour map of the base of the transported regolith (contour interval 10 metres)

granules tend to decrease in abundance whilst the amount of lateritic debris increases.

The colluvial blanket has incised into the lacustrine clay facies of the palaeochannel sediments and the lateritized Archaean basement. The base of the colluvium forms a broad valley that mimics the one occupied by the palaeochannel and implies an alluvial component to sediment deposition (Fig. 4.4). The estimated minimum thickness of stripped material is in the order of 15 metres over the centre of channel. This gradually diminishes to very minimal incision about half way up the valley sides where a complete in-situ laterite profile within Archaean rocks is present beneath the colluvium (Figs. 4.6, 4.7, 4.8).

There is extensive development of a basal gravel within the colluvium/alluvium. It is composed of abundant lateritic debris, of which the particular component mix depends largely on the available regolith material.

On the upper valley slopes where lateritic residuum over Archaean basement has been exposed to colluvial action, the basal gravels are primarily composed of similar material (pisolitic and nodular laterite; most with intact cutans). The laterite rich basal unit tends to lens down slope towards the channel centre before dissipating. This occurs shortly after passing the point where the lacustrine clay facies of the palaeochannel onlaps the pre-Eocene laterite profile, thus denying the supply of new lateritic material (Figs. 4.6, 4.7, 4.8).

Where the colluvium/alluvium overlies the lacustrine clays, the basal gravel reverts back to a more polymict nature. Ferruginous granules, cutaneous lateritic pisoliths and nodules, and spherical pisoliths are the most abundant components (Fig 4.9C). The spherical pisoliths are not likely to have formed in-situ within the colluvium, but are instead probably derived from the abraded lacustrine clays.

The colluvium/alluvium has also incised subsidiary gullies parallel to and above the trace of the Avoca Shear (adjacent to the points where the palaeochannel enters and leaves the same shear zone) (Fig. 4.4). These erosional trends are again also mimicked by the underlying palaeochannel where subsidiary gullies are elongated along the shear zone to the north-west and south-east (Fig 4.3).

4.2.3 Lacustrine clay

The lacustrine clay sediments are correlatable to the lacustrine clay facies at Gindalbie and to the Perkolilli Shale described by Kern & Commander (1993) mainly from within the trunk channels of the Roe Palaeodrainage system. They conformably overlie the sand facies and lenses of colluvial/alluvial lateritic detritus on the channel margins.

The clays are uniform and generally featureless. They are red-brown coloured, generally oxidized and not at all similar to Gindalbie where reduced clays are ubiquitously developed. Ferruginous products within the clay are also not as well developed as within the oxidized clay at Gindalbie. However, spherical pisoliths and related ferruginous nodules are reasonably well developed in some horizons (Fig. 4.10 E & F). Sections of numerous spherical pisoliths revealed them to be accreting on other ferruginous granules and pisoliths. No evidence was found of pisoliths accreting on fossil plant material as was the case at Gindalbie.

The clays often contain a basal lag of lateritic detritus especially on the channel margins. The lag often persists into the underlying sand facies at the same locations.

4.2.4 Fluvial sand

The fluvial sand is correlatable to the Wollubar Sandstone of Kern & Commander (1993) and to the sand facies at Gindalbie. It is identical to the Gindalbie sand in terms of composition, grading, and (lack of) weathering overprint.

The sand is poorly sorted, angular and of quartz composition. It has a fining - upwards gradation with a coarse basal gravel and is almost certainly derived from the granite terrain approximately 7 km to the north-east.

The sand occupies only the deepest portion of the palaeochannel and grades to a kaolinitic clay rich facies on the channel flanks. Interfingers of lateritic detritus are commonly present within the sand facies profile on the channel margins (section 4.2.2)

4.2.5 Pre-Eocene regolith

The palaeochannel has incised into a pre-existing deeply weathered (lateritized) Archaean basement. Preservation of the underlying laterite profile is extensive on the upper banks and periphery to the channel. The Kurnalpi site is further from the local depocentre of the main trunk palaeoriver than the Gindalbie site and as a result less stripping of the pre- Eocene landform has occurred relative to the latter.

The idealized Yilgarn laterite profile of Anand & Smith (1993) is applicable at Kurnalpi: An upper unit of pisolitic and nodular lateritic residuum overlies a zone of ferruginous saprolite. This in turn overlies a partially leached saprolite which gradually grades through to saprock then finally bedrock. The relative proportions of each component can be gauged from the three cross sections across the channel (Figs. 4.6, 4.7, 4.8).

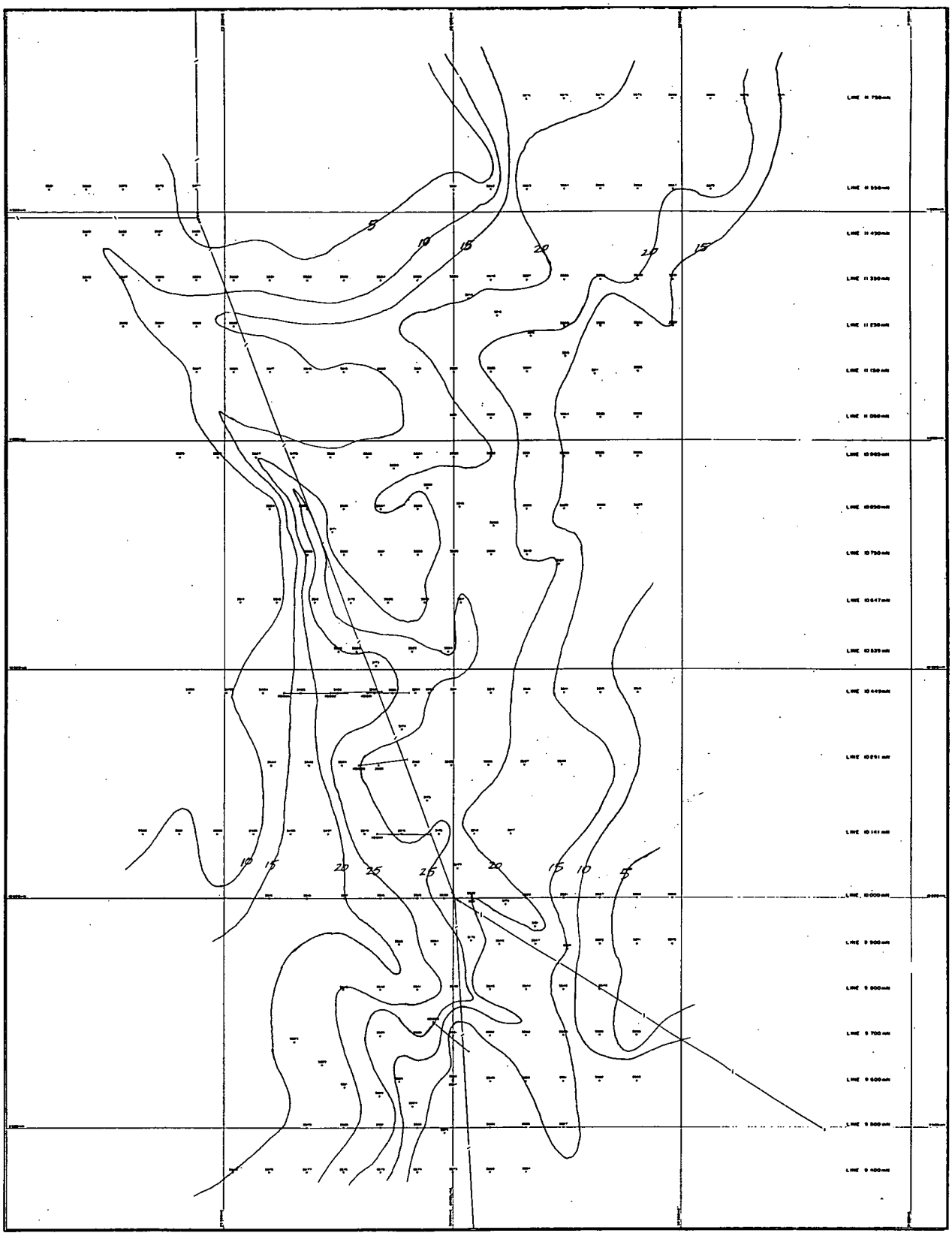

Figure 4.4 Contour map of the base of the colluvium/alluvium (contour interval 5 metres)

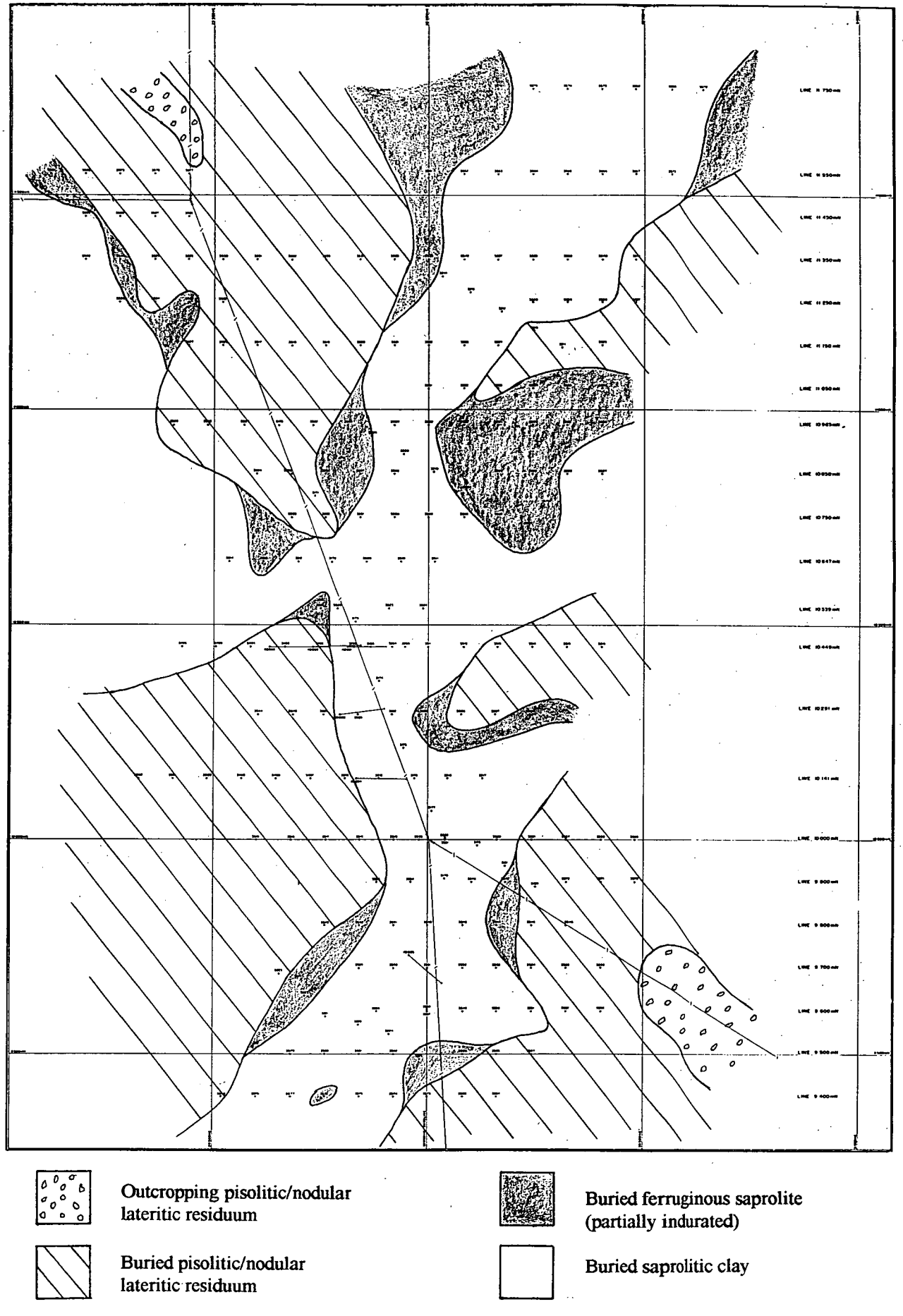

Figure 4.5 Pre-Eocene regolith facies at the palaeochannel unconformity.

Moving across the channel profile away from the thalweg position successively higher components of the laterite profile are preserved.

1. The deepest portions of the palaeochannel have incised to the partially leached saprolite below the ferruginous zone of the laterite profile, yet is at least still 20 metres above the saprock/bedrock weathering front (Fig. 4.5). The saprolitic clay, when developed after komatiite, is uniformly massive, textureless, non-indurated, and retains some bedrock colouration. Where the channel thalweg overlies basalt, ferruginization of the lower regolith is more intense, resulting in substantial Fe-induration (also the preferred location of supergene/bedrock gold mineralization).

2. Ferruginous saprolite (with the upper-most component of pisolitic lateritic residuum stripped away) is preserved as a band between a third and half way up the channel sides (Fig. 4.5). It is partially indurated by goethite and kaolinite replacement of original mineralogy (Anand & Smith, 1993), with a distinct brown-yellow colour. Bedrock textures are often preserved (notably spinifex texture in komatiite)

3. The full laterite profile with sand and clay facies on-lap (especially in the south) is preserved within the upper half of the channel profile (Fig. 4.5). Up to 10 metres of pisolitic and nodular lateritic residuum is generally underlain by sequentially, ferruginous saprolite, leached saprolite, and saprock/bedrock. The full laterite profile is preserved in most areas adjacent to the channel, and in fact crops out in the north-west and south-east. Though in the western-central portion of the study area the top of the laterite has been stripped back to saprolite by colluvial/alluvial action (Fig. 4.7)

Further evidence that the channel has incised into a pre-existing laterite profile is the presence of discrete horizons of pisolitic and nodular lateritic debris contained within both the sand and clay facies of the palaeochannel. They occur only on the channel margins adjacent to the point where stripping of the upper unit of the in-situ laterite profile first occurs (Figs 4.9 C & D, 4.6, 4.7, 4.8) . The presence of this material within the channel sediments constrains the relative timing and landform relationships.

An alternative hypothesis for the origin of this lateritic material is that it has developed in-situ as a result of post-Eocene lateritization of the palaeochannel sediments. This scenario can be rejected on the basis of the distribution pattern of the lateritic material within the sediments: ie.

- It is absent over the deeper middle sections of the palaeochannel.
- It is confined to discrete semi-continuous horizons, at separate stratigraphic positions within the sediments
- It is spatially related to the presence of in-situ pre-Eocene laterite on the channel margins.

Drillhole intercepts of the pre-Eocene weathering profile indicate that lateritization of the bedrock occurred within an already existing broad shallow valley that was of similar dimensions to the one occupied by the palaeochannel/colluvial sediments. Reconstruction of the partially and progressively stripped laterite profile indicates that the prior valley sides have an approximate slope of 3-4 degrees (slightly flatter than that occupied by the palaeochannel), and that the palaeochannel has incised a maximum of 25 - 30 metres of lateritized Archaean basement (Figs. 4.6, 4.7, 4.8).

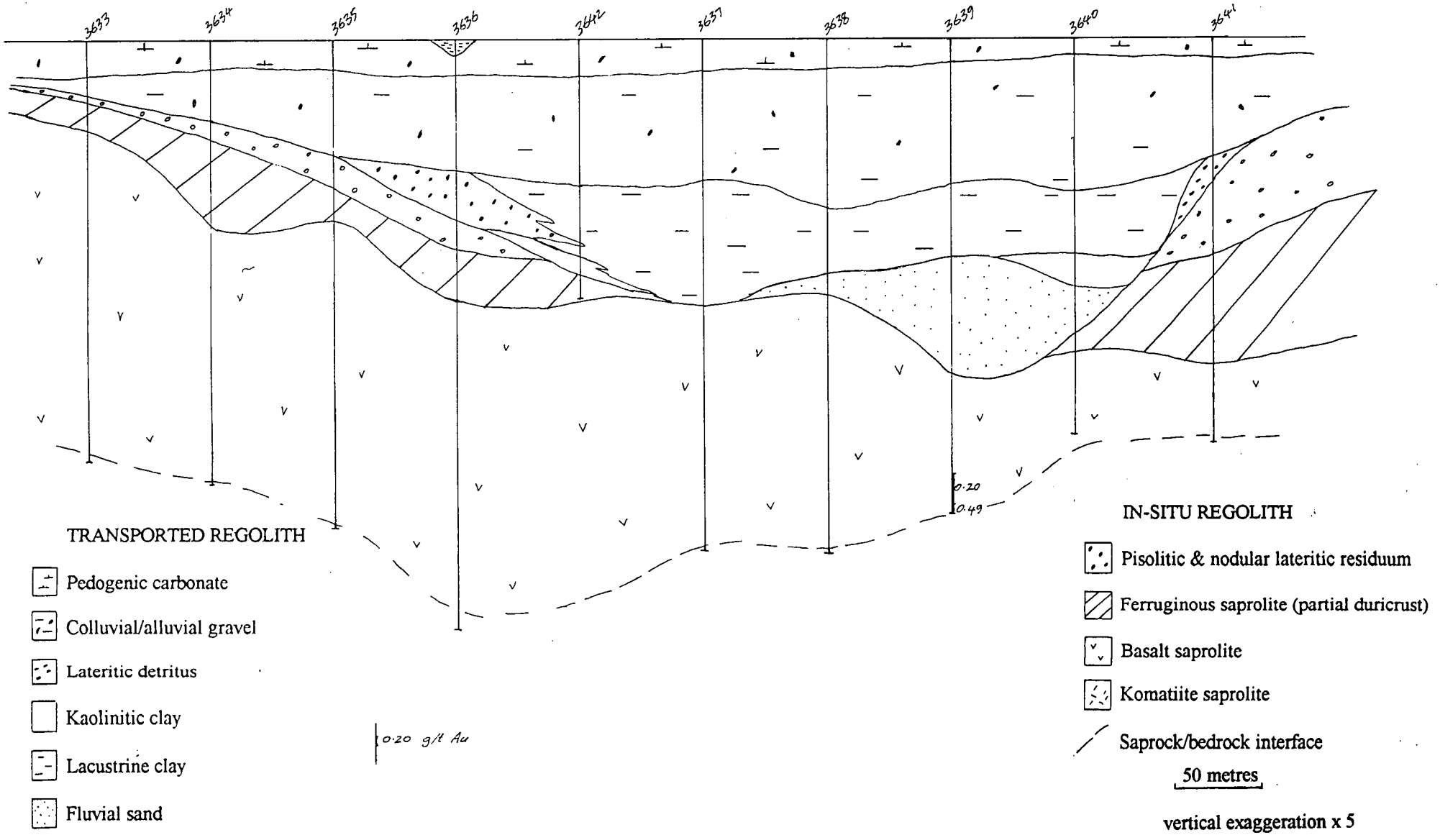

Figure 4.6 Cross section along the 11350 mN line; northern section

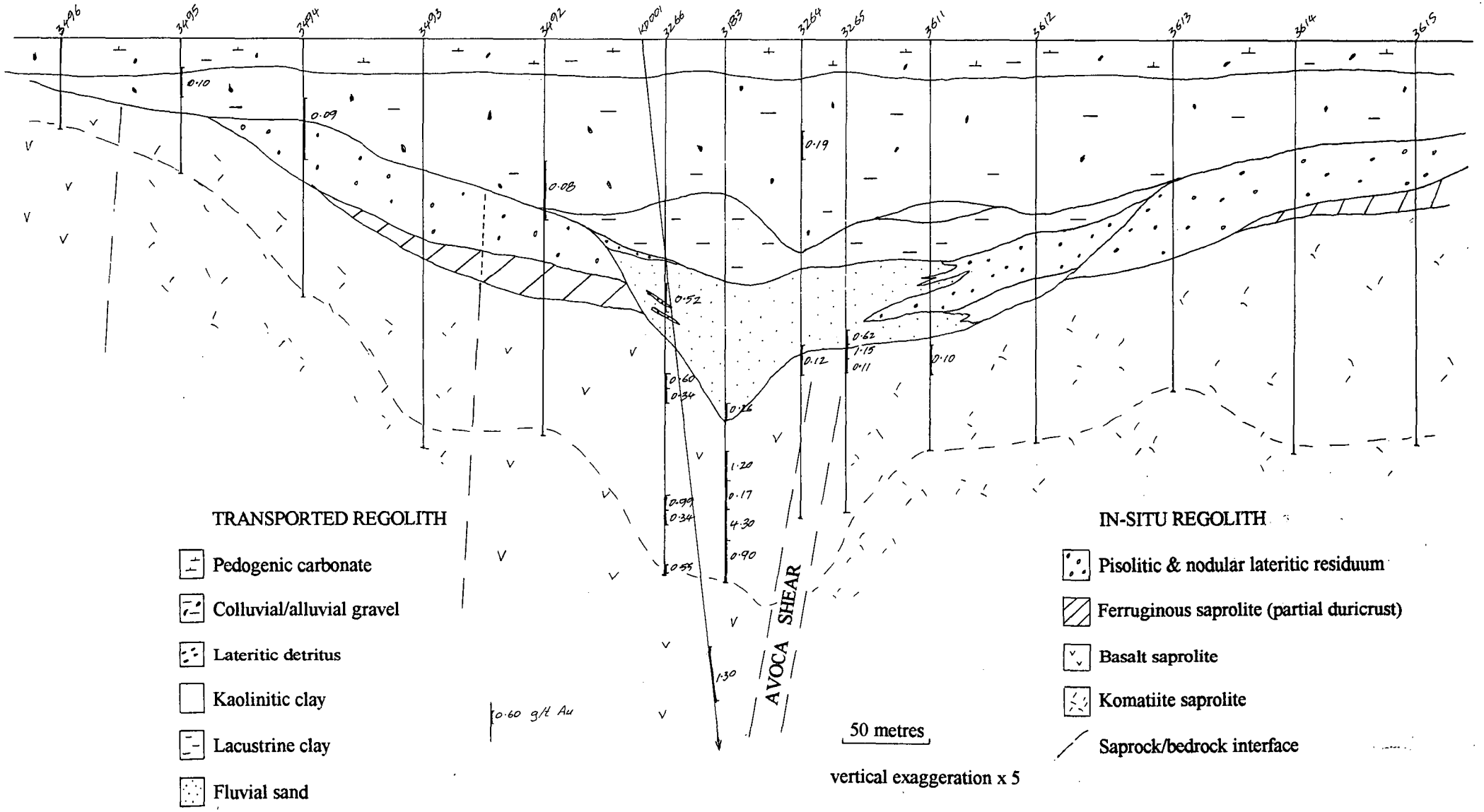

Figure 4.7 Cross section along the 10449 mN line; central anomaly

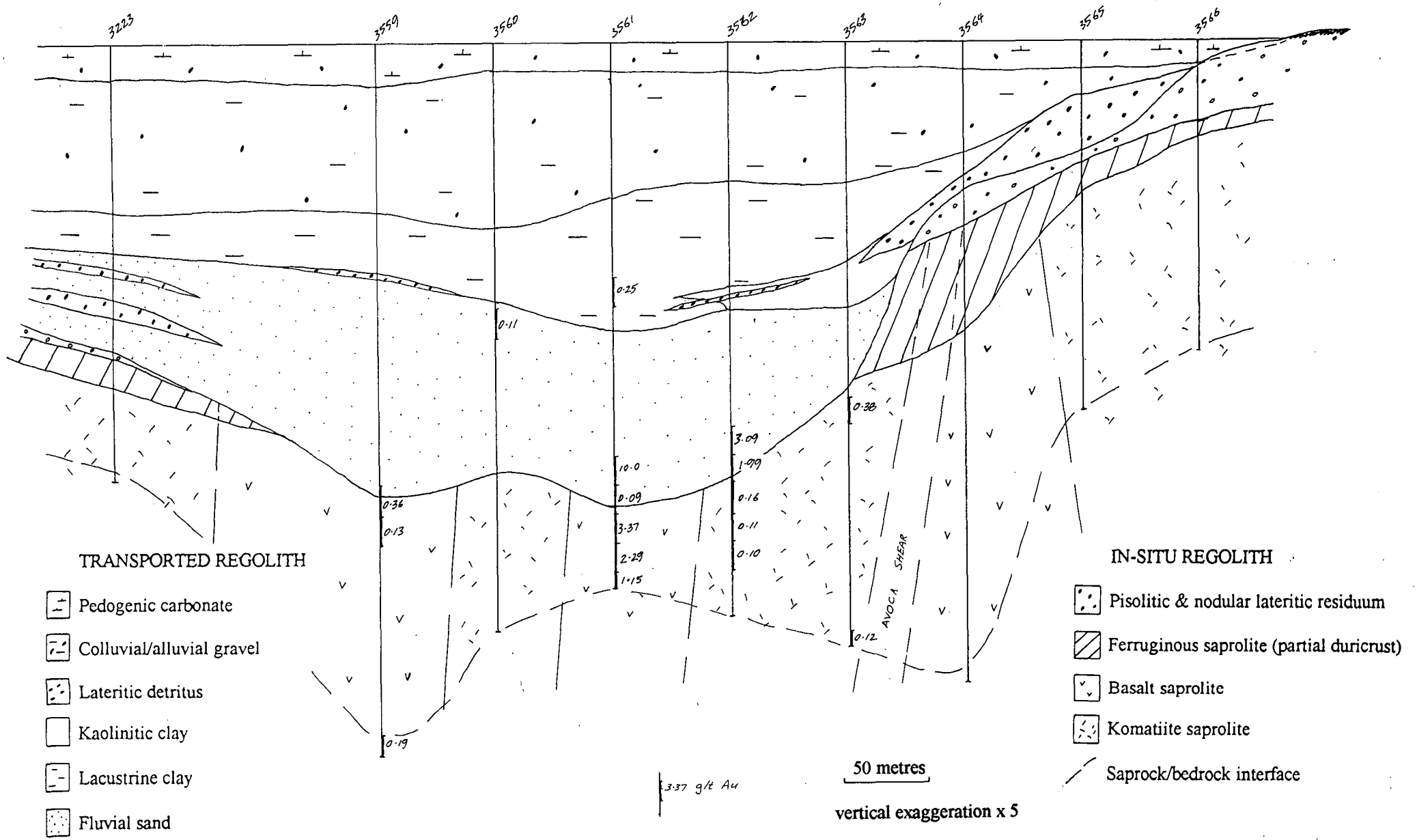

Figure 4.8 Cross section along the 9700 mN line; southern anomaly

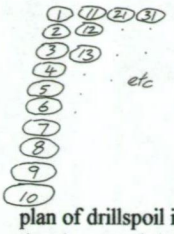

plan of drillspoil intervals for
the photo at right
drillspoil collected over 1 metre
intervals

TYPE SECTION - WESTERN CHANNEL MARGIN
KSC 3209 29865E 10940N

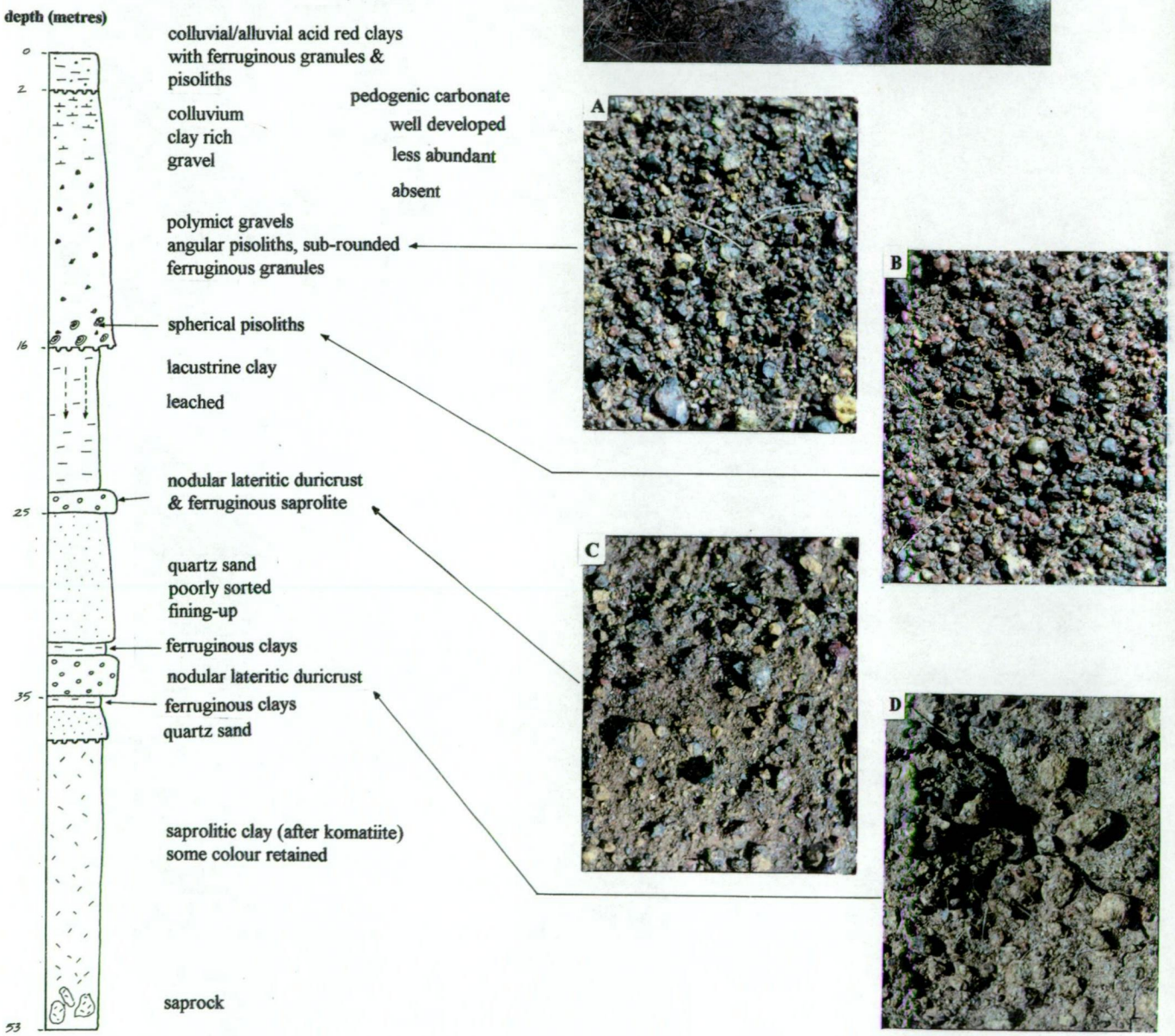

Figure 4.9 Type section through channel periphery - based on hole KSC 3209
(top photo shows drillspoil arranged in 1 metre piles)
A. polymict colluvial gravel
B. polymict colluvial gravel with abundant spherical pisoliths
C. & D. transported lateritic debris (limited transport)

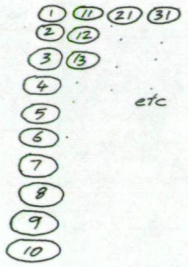

plan of drillspoil intervals for the photo at left
drillspoil collected over 1 metre intervals

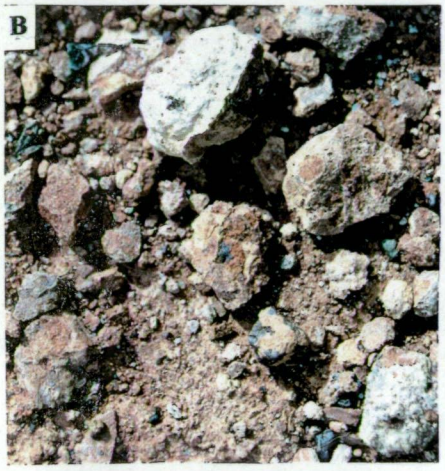

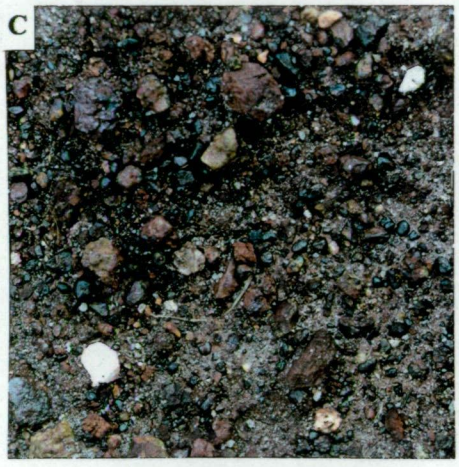

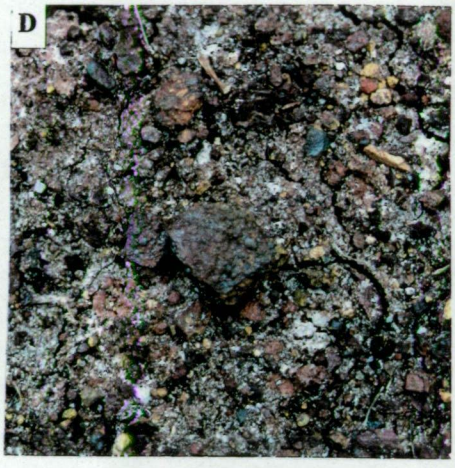

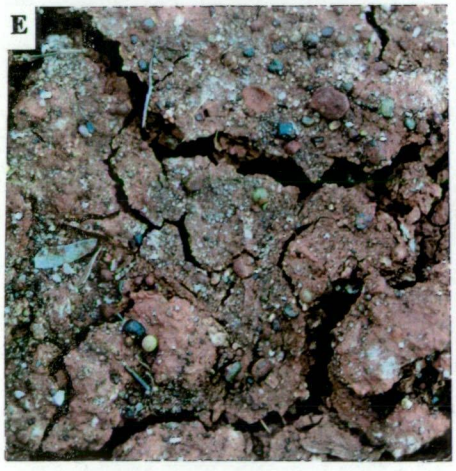

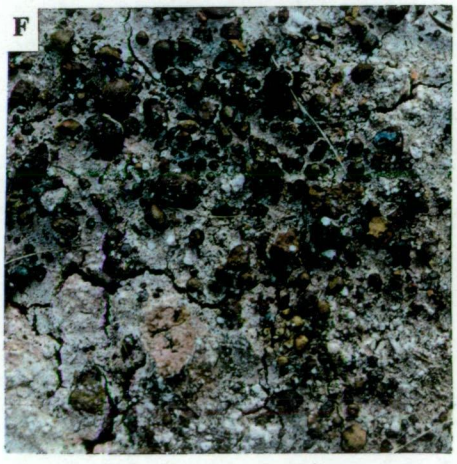

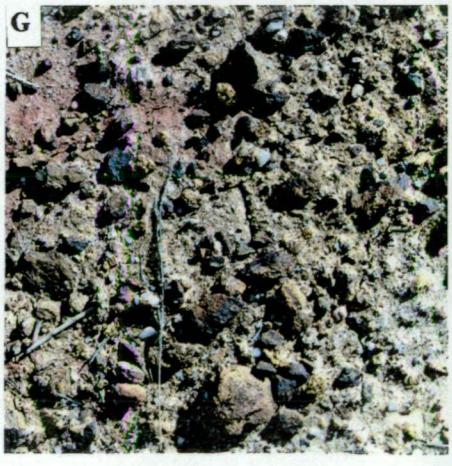

Figure 4.10 Some examples of regolith features from hole KSC 3183 (channel thalweg, central anomaly)

A) overview of drillspoil. B) pedogenic carbonate from the first 4 metres. C) polymict colluvial/alluvial gravel at 18m depth. D) polymict colluvial/alluvial gravel with secondary Fe cementation at 20m depth. E) lacustrine clays with spherical pisoliths at 27m depth. F) fluvial sand with lateritic nodules and spherical pisoliths at 32m depth. G) lateritized ferruginous saprolite below the palaeochannel at 53m depth.

4.4 Gold mineralization

4.4.1 Overview

Gold mineralization within the study area is almost exclusively confined to the palaeochannel or to the Avoca Shear - palaeochannel juxtaposition, and can be divided into 2 spatial associations:

(a) gold located within the palaeochannel sediments or at the unconformity with the Archaean saprolite (Fig. 4.11)

(b) gold located within the Archaean saprolite/bedrock (Fig. 4.12).

Gold distribution patterns for each of the two categories are virtually coincident. There is a broad anomalous zone of gold mineralization some 1500 metres long within the regolith (both transported and residual) at the palaeochannel - Avoca Shear juxtaposition. Within this broad zone there are two main anomaly peaks that encompass both mineralization categories:

A central anomaly located between 10200N and 10500N, and a southern anomaly located on a prominent bend in the palaeochannel between 9550N and 9750N. Relatively high grade mineralization is developed in both the basement regolith (generally beneath the channel thalweg) and within palaeochannel sand at or near the unconformity. Sediment hosted gold mineralization peaks tend to lie adjacent to and slightly offset from corresponding peaks within basement material (Figs. 4.11, 4.12).

4.4.2 Gold mineralization within palaeochannel sediments

Most palaeochannel hosted gold mineralisation is located at the base of the sand, on the unconformity, and extending a few metres into the upper saprolite. The highest grades are located at the unconformity at the base of the channel (Table 4.2).

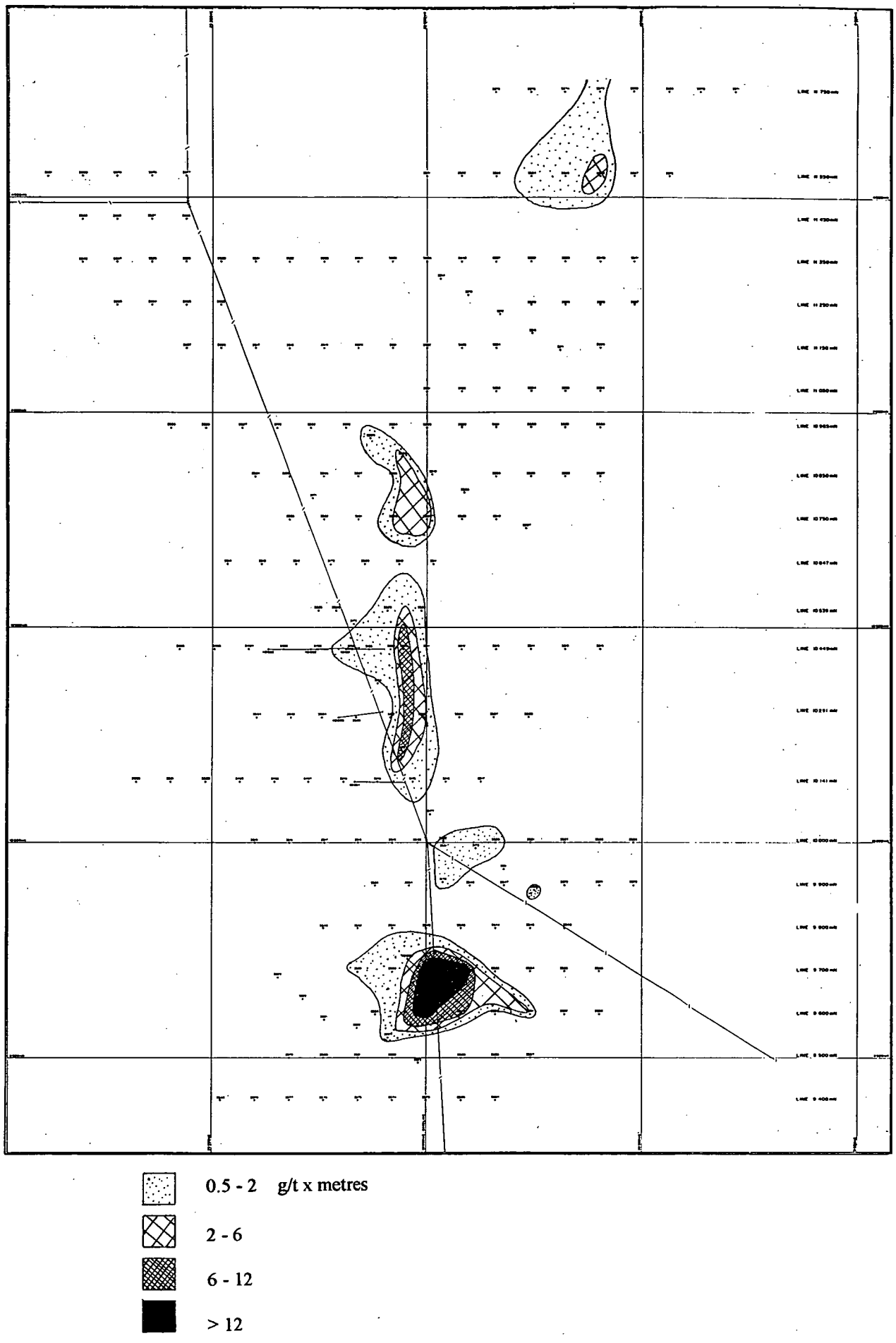

Figure 4.11 Anomalous gold within the transported components of the regolith; mainly at the base of the palaeochannel (grams per tonne x metres).

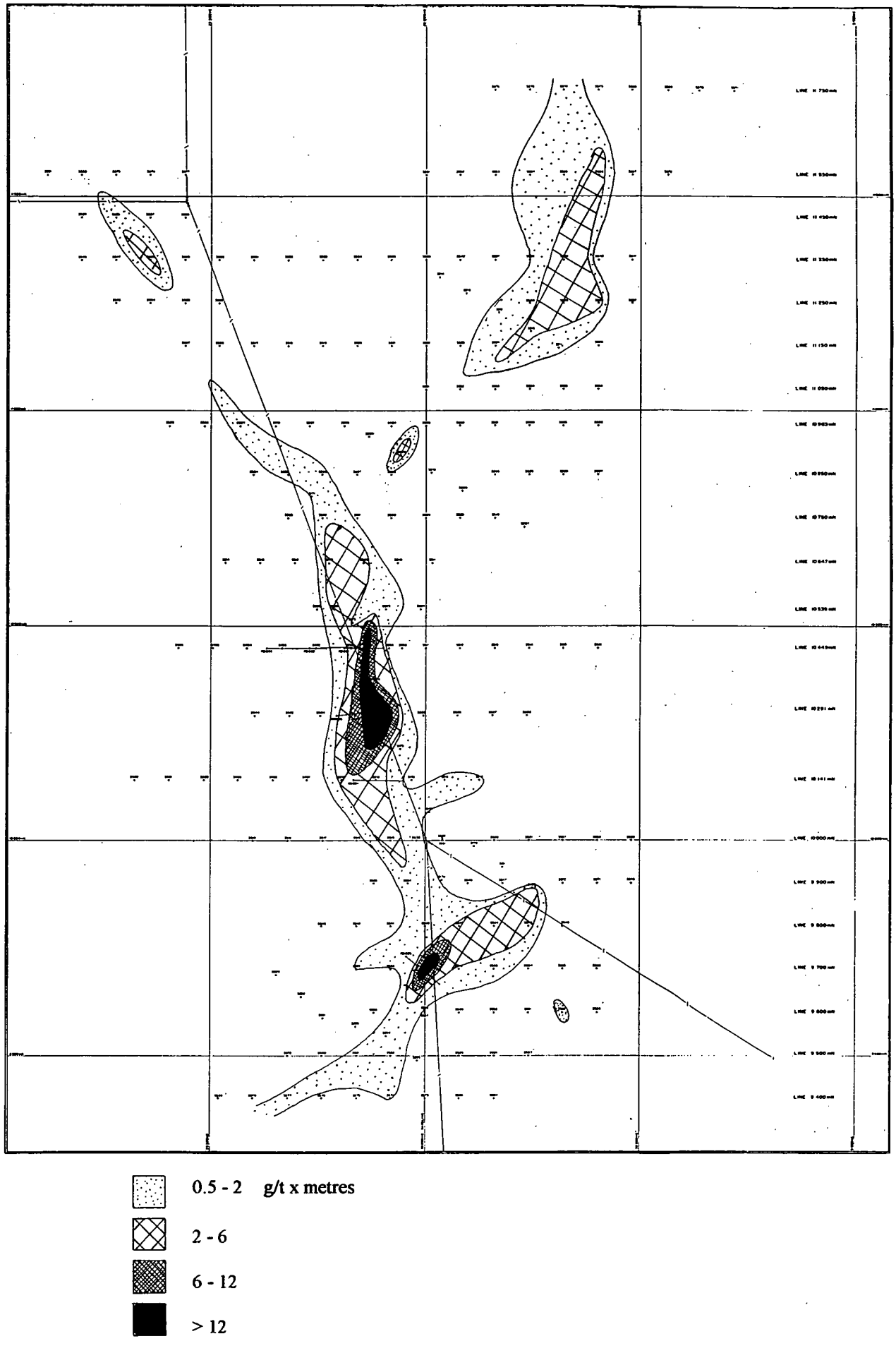

Figure 4.12 Anomalous gold within the in-situ components of the regolith; mainly within ferruginous mafic saprolite (grams per tonne x metres).

Some minor mineralisation is located within the sand and clay facies as well as the overlying colluvium though most occurrences are sporadic and are not correctable from hole to hole.

Both the high grade and minor gold trends are spatially related to the palaeochannel thalweg. The highest gold grades tends to be either at or adjacent to the thalweg position, and minor mineralization at higher stratigraphic levels tends to be directly above the channel thalweg.

DRILLHOLE NO.	CO-ORDINATES	ANOMALOUS Au INTERSECTIONS	LITHOLOGICAL CONTROL ON MINERALIZATION
	CENTRAL	ANOMALY	
KSC 3175	29940E 10215N	4m @ 2.04 g/t from 52m	palaeochannel/saprolite unconformity
KSC 3265	29945E 10450N	4m @ 0.99 g/t from 38m	palaeochannel/saprolite unconformity
KSC 3505	29995E 10290N	8m @ 0.28 g/t from 40m	palaeochannel/saprolite unconformity
	SOUTHERN	ANOMALY	
KSC 3561	30000E 9700N	4m @ 10.80 g/t from 56m	base of sand
KSC 3562	30080E 9700N	8m @ 2.54 g/t from 52m	lower sand
KSC 3558	30000E 9600N	4m @ 8.36 g/t from 60m	palaeochannel/saprolite unconformity
KSC 3549	30080E 9600N	2m @ 1.66 g/t from 58m	palaeochannel/saprolite unconformity
KSC 3551	30240E 9600N	12m @ 0.41 g/t from 48m	base of sand

Table 4.2 Significant gold mineralization within the palaeochannel sediments.

4.4.3 Gold mineralization within basement regolith/bedrock

The gold anomaly within the basement regolith tends to be more cohesive than the palaeochannel-hosted mineralization and is spatially associated with the following items: (Figs. 4.2, 4.3, 4.12)

i.) mineralization tends to be contained in mafic rocks

ii.) mineralization tends to be developed below the palaeochannel

iii). the main mineralization trend is developed on or adjacent to the Avoca Shear

The saprolite/bedrock mineralization is generally located beneath the palaeochannel with the best grades adjacent to or beneath palaeochannel hosted gold

peaks. Two trends are evident; - one immediately beneath the channel thalweg, the other elongated along the trace of the Avoca Shear. Where all three spatial associations (above) are coincident the highest gold grades are encountered (Fig 4.12 & Table 4.1).

DRILLHOLE NO.	CO-ORDINATES	ANOMALOUS Au INTERSECTIONS	LITHOLOGICAL CONTROL ON MINERALIZATION
	CENTRAL	ANOMALY	
KSC 3174	29885E 10370N	6m @ 0.54 g/t from 56m	saprolite/saprock interface
KSC 3182	29915E 10290N	8m @ 1.83 g/t from 48m	upper saprolite
KSC 3183	29865E 10450N	8m @ 1.67 g/t from 54m	whole of saprolite
KSC 3503	29835E 10290N	8m @ 0.85 g/t from 52m	saprolite/saprock interface
KSC 3515	29920E 10000N	11m @ 0.82 g/t from 52m	lower saprolite
KSC 3218	29885E 10140N	11m @ 0.47 g/t from 54m	lower saprolite
KSC 3219	29805E 10140N	3m @ 1.20 g/t from 68m	saprolite/saprock interface
KSC 3266	29825E 10450N	4m @ 0.67 g/t from 60m	whole of saprolite
KSC 3526	29787E 10539N	4m @ 0.96 g/t from 36m	upper saprolite
KSC 3172	29775E 10650N	4m @ 0.85 g/t from 40m	upper saprolite
KSC 3509	29855E 10650N	4m @ 1.11 g/t from 48m	whole of saprolite
	SOUTHERN	ANOMALY	
KSC 3561	30000E 9700N	10m @ 2.15 g/t from 64m	whole of saprolite
KSC 3543	30080E 9800N	4m @ 1.18 g/t from 76m	saprolite/saprock interface
KSC 3544	30160E 9800N	4m @ 0.65 g/t from 48m	upper saprolite
KSC 3545	30240E 9800N	4m @ 0.63 g/t from 40m	upper saprolite
KSC 3180	30250E 9890N	8m @ 0.61 g/t from 64m	lower saprolite

Table 4.1 Significant gold mineralization within saprolite at Kurnalpi (all intersections are located at the palaeochannel/Avoca Shear juxtaposition).

The best drillhole intersection is from the central anomaly (drillhole KSC 3183 :-17 metres @ 1.67 g\t Au from 54 metres) and is located in highly weathered, ferruginous basalt saprolite. The mineralization is associated with abundant fe-oxide pseudomorphs after pyrite, vein quartz and halloysite clay. This zone is interpreted as being the oxidized portion of the lode-style trend intersected at depth by diamond drilling.

Subsequent deep diamond drilling under the central anomaly intersected a gold bearing, intensely altered (bleached\silica\fuchsite) quartz stockwork within hangingwall basalts adjacent to the Avoca Shear. Gold is disseminated as small blebs in pyrite (and minor sphalerite) contained within quartz veins (S. Goertz, pers.

comm. 1994). Further drillholes under the southern anomaly and south of the central anomaly failed to detect significant bedrock mineralization.

DRILLHOLE NO.	CO-ORDINATES	ANOMALOUS Au INTERSECTIONS	LITHOLOGICAL CONTROL ON MINERALIZATION
	CENTRAL	ANOMALY	
KD 001	29810E 10449N	low level gold (< 0.5 g/t)	sand facies of palaeochannel
		7m @ 1.30 g/t from 80m	oxidized qz veins within partly weathered bleached basalt
KD 002	29730E 10449N	7m @ 0.15 g/t from 113m	qz veins within basalt
		27m @ 0.41 g/t from 124m	qz veins within basalt (main bleached zone)
KD 003	29790E 10291N	15m @ 0.52 g/t from 60m	ferruginous basaltic saprolite/saprock
KD 004	29830E 10141N	5m @ 0.40 g/t from 116m	chlor/fuchsite altered basalt
KD 006	29930E 10449N	7m @ 0.29 g/t from 156m	qz veins within basalt
		2m @ 0.53 g/t from 168m	qz veins within basalt
		9m @ 0.29 g/t from 190m	qz veins within basalt (main bleached zone)
		4m @ 1.53 g/t from 236m	qz veins within mafic rock
	SOUTHERN	ANOMALY	
KD 005	29954E 9730N	nil	

Table 4.3 Significant gold mineralization within diamond drillholes at Kurnalpi (all drillholes are located at the palaeochannel/Avoca Shear juxtaposition).

4.5 SEM analysis of gold grains

A number of free gold grains from the base of the sand at the southern anomaly were collected for analysis. The purpose was to observe the morphology of the grains and to determine the silver content of the gold. The base of the palaeochannel at this site contains the strongest mineralization in the study area. It is also the furthest downstream extent of mineralization within either the transported or saprolitic components of the regolith.

A dozen or so gold grains were collected from the base of the palaeochannel in hole KSC 3558. The grains were collected from was 60-61 metres interval, which is the metre of sand directly above the unconformity. In this hole the anomalous

intersection is 4 metres @ 8.47 g/t from 60 metres (the gold grade of drillholes has been assayed over four metre intervals).

Six grains, ranging in size from 280 μm to 560 μm, were selected at random for SEM analysis. All the grains show evidence of rounding presumably as a result of mechanical transport within the channel. A number of the grains also exhibit probable xenomorphic faces with evidence of striae; suggesting growth adjacent to pyrite crystals (Fig. 4.13 E, F).

Energy dispersive analysis of the grains attempted to quantify the presence of impurities within the gold, in particular the presence of Ag. The analyses were performed on the surface of the grains and no data on the internal composition has been gathered. Energy dispersion histograms and semi-quantitative analyses for each grain are presented in figure 4.14.

Specimens (B), (D) and (E) have superficial compositions with significant Ag (1.6 to 2.3 weight %). Specimens (A) and (C) appear to contain no superficial Ag.

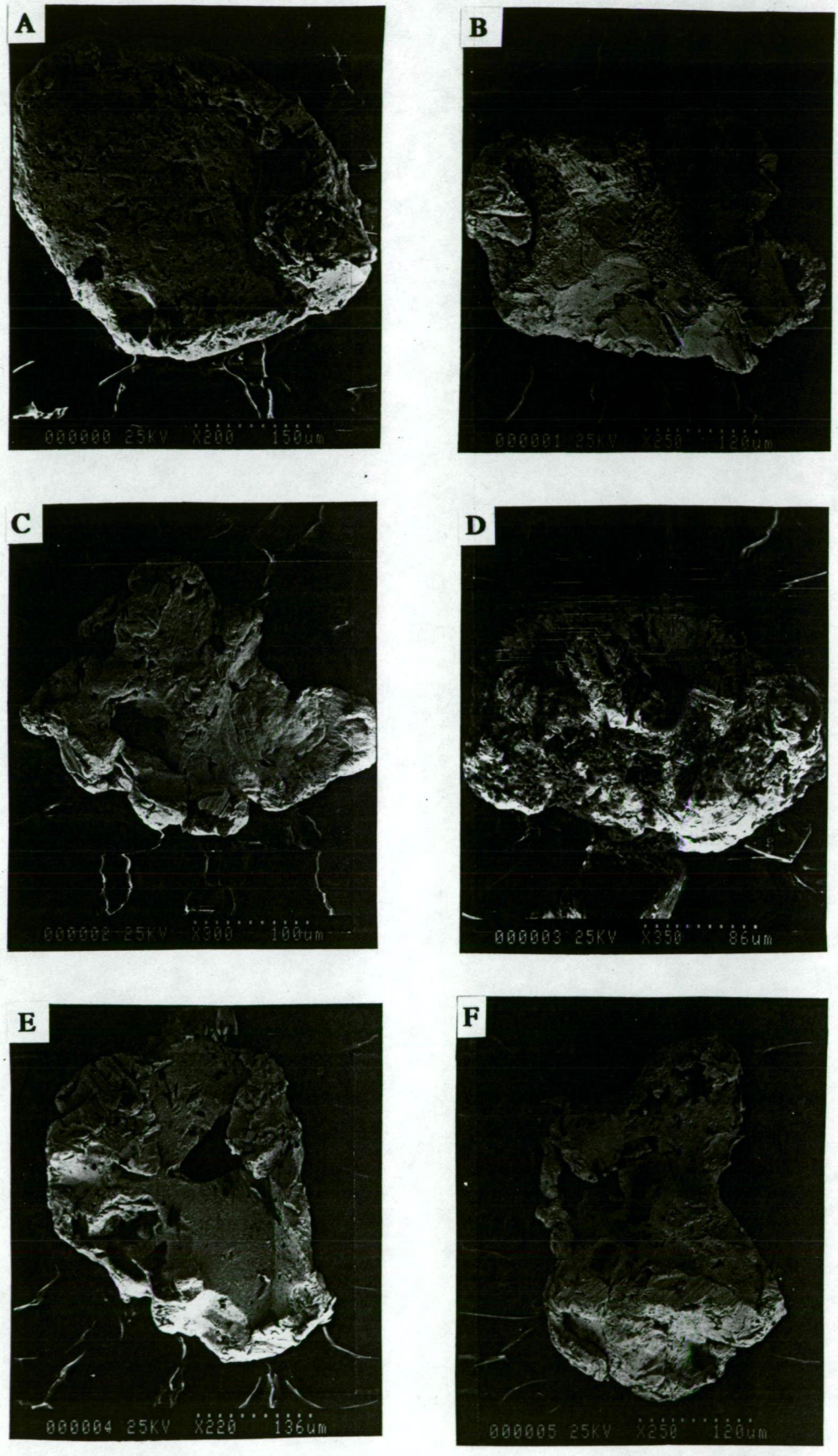

Figure 4.13 Scanning electron micrographs of six gold grains from the base of the palaeochannel (drillhole KSC 3558). All grains show some rounding. E & F exhibit probable xenomorphic crystal faces with possible striae after pyrite.

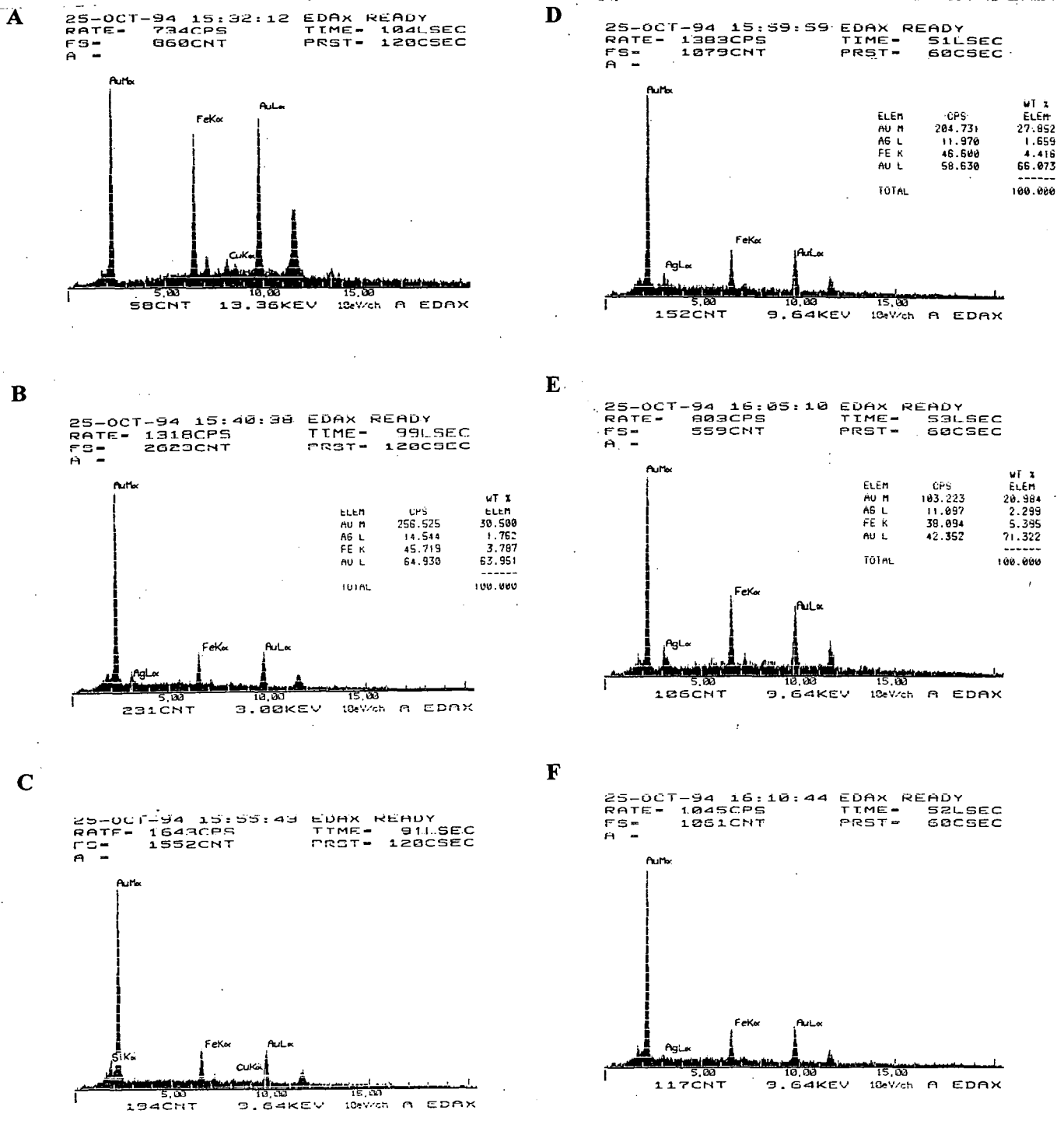

Figure 4.14 SEM energy dispersive analyses of gold grains A to F from Figure 4.13. Grains B, D & E show significant Ag contents up to 2.3 wt %.

5.0 DISCUSSION

5.1 Regolith formation and relative timing

5.1.1 Lateritization

The Gindalbie and Kurnalpi study areas are located over different greenstone assemblages and different drainage regimes, but investigations at both sites indicate a number of consistent patterns in regolith landform relationships and formation history in the Kalgoorlie area.

At both study areas two separate lateritization events are preserved within the regolith. One within pre-palaeochannel basement, the other within the palaeochannel sediments. The lateritization of the basement rocks is partially litho-dependant, with intense leaching of the lower profile more prevalent in felsic rocks (Gindalbie), and intense ferruginization of the upper profile more prevalent in mafic and to a lesser extent ultramafic rocks (Kurnalpi).

The initial lateritization event has occurred prior to palaeochannel incision but within a landscape already incised by at least north-south oriented valleys (Kurnalpi) - most likely the result of Permian glaciation (Ollier et al. 1988). van de Graaff and others (1977) also report a palaeochannel contained within a Permian glacial valley near Ponton Ck. east of Kalgoorlie. Bird & Chivas (1993) use oxygen-isotope data to argue for a widespread pre-Late Mesozoic lateritization event over Eastern Australia. Though very limited data from Western Australia does not support this date, it is likely that such a widespread event would apply to the Kalgoorlie region.

The laterite profile recognised by Anand & Smith (1993) from numerous regions of the Yilgarn is typified by this earliest lateritization event. The terminology

used to describe the laterite stratigraphy is that developed by Anand and others (1993). The pre- Eocene event was much more intense than the one developed within the Eocene palaeochannel sediments. The complete upper profile of pisolitic and nodular ferruginous duricrust is only developed in the pre-Eocene event. The later lateritization has only relatively minor ferruginization of the upper profile.

The development of the post-Eocene laterite profile is likely to be a regional event and is best observed at Gindalbie where it is complete and intact. Apart from developing a ferruginous upper profile, the later lateritization event has resulted in further deep weathering beneath the palaeochannels; - probably in the order of 10 - 20 metres. At Kurnalpi incision by latter colluvium has removed the top 15 to 20 metres of the lacustrine clays (the easily identifiable ferruginous component) thus making identification of the later profile difficult; - on the valley sides it has overprinted the more intense pre-Eocene laterite, again masking ready identification. The base of the colluvium contains abundant spherical pisoliths almost certainly developed within the lacustrine clays and indicating that the ferruginous upper profile was at some stage in the past developed at Kurnalpi as well. Kern & Commander (1993) also report ferruginization of the upper horizons in the main trunk channels of the Roe Palaeodrainage, and profiles similar to that at Gindalbie have been observed in pit walls at QED at Kanowna (R. Anand pers. comm. 1993) and at LBE.

The colluvium at both Gindalbie and Kurnalpi appears to have undergone little or no ferruginization, except for minor Fe induration at the base at the Kurnalpi site. Also, given that it has truncated the likely lateritized lacustrine clay at Kurnalpi, colluvium development has most probably occurred during the waning stages of the post-Eocene lateritization event and up to the present.

The final regolith modifying process is the ubiquitous development of pedogenic carbonate in the top 2 - 5 metres at both sites. Only small presently active alluvial washes have no carbonate induration and in fact truncate the carbonate profile in the colluvium.

5.1.2 Palaeochannel incision

By reconstructing the laterite profile across the palaeochannel valleys, the depth of incision by the palaeochannels is 40 - 50 metres at Gindalbie, and 25 - 30 metres at Kurnalpi. These relative depth differences are the result of the Kurnalpi site being further from the main trunk channel than Gindalbie. In both cases though the channel thalwegs have much steeper gradients then the trunk channels; - about 8 metres per km at Kurnalpi and about 2.2 metres per km at Gindalbie, compared with < 1 metre per km in the eastern Roe palaeodrainage (Kern & Commander 1993).

The trunk channels have incised to a maximum depth of 20 metres beyond that at Gindalbie (Commander et al. 1991); Thus the maximum total depth of incision of the Roe Palaeodrainage into the underlying weathered Archaean basement is in the order of 70 metres.

The Kurnalpi study area also provides evidence of substantial stripping of both the palaeochannel sediments and the pre-channel regolith by relatively recent colluvial action. The colluvium has completely stripped the ferruginous upper profile in the central - west of the study area; - probably 15 - 20 metres (Fig 4.7). This certainly demonstrates the potential for substantial truncation of the pre-Eocene laterite profile at least on upper slopes in the Kalgoorlie region.

The partially truncating colluvial process is the result of continued uplift about the Jarrahwood Axis coupled with the onset of aridity. Clarke (1994a, 1994b)

reports that gypsum deposits in the Cowan and Lefroy palaeochannels establish the onset of aridity at least since the Early Pliocene. Thus a tentative framework for the timing of regolith formation is:

1. Permian glaciation establishing at least north-south trending valleys
2. Mesozoic deep weathering resulting in an extensive laterite profile
3. Pre-Middle Eocene palaeochannel incision over the relatively intact laterite profile resulting in complete stripping of the upper profile in lowland areas
4. Late Eocene to Early Pliocene lateritization
5. Post Early Pliocene secession of lateritization, but development of substantial colluvial action resulting in extensive partial truncation of pre-existing regolith on upland areas
6. Recent development of pedogenic carbonate

5.2 Gold mineralization

Gold distribution patterns at both study areas are heavily influenced by the presence and morphology of the palaeochannels. In both cases the highest gold grades are biased about a vertical plane through the channel thalweg.

5.2.1 Gindalbie

At Gindalbie basement mineralization is apparently not present. Gold distribution is caused by chemical mobilization and precipitation along favourable horizons within the palaeochannel sediments. Gold is preferentially deposited within the reduced clay along the tributary channel (equivalent to the "hanging passive front" of Smyth & Button 1989), and within the reduced clay and at the basal

channel contact with sulphidic carbonaceous shales in the main channel. There is also no gold distributed at the main (present) redox boundary which suggests that the gold is not carried as a chloride complex but as a thiosulphate complex. (Lawrance 1990, 1993, Mann 1984).

Analysis of spherical pisoliths at the main redox front indicates that there is no anomalous concentration of chalcophile elements (or Au) at this boundary. However sample SL210, recovered from a moderately Au anomalous horizon within the reduced lacustrine clay, has distinctly anomalous mobile chalcophile element concentrations and slightly anomalous gold concentrations. The relatively high Mn level in this sample suggests that elevated manganese levels may be present within the reduced clay at this horizon and may be controlling Au precipitation.

5.2.2 Kurnalpi

Gold distribution within the regolith at Kurnalpi is controlled by a) basement lode mineralization; and b) palaeochannel location and morphology.

The majority of the gold is distributed at either the base of the channel sand or within the saprolite directly beneath it. Lode-style mineralization at the central anomaly is truncated by the palaeochannel resulting in virtually coincident transported and in-situ regolith anomalies. Similar gold distribution patterns are present at the southern anomaly, but at this stage no bedrock mineralization has been located beneath it.

Gold grains recovered from the base of the sand at the southern anomaly display probable xenomorphic features suggesting a primary origin. Gold precipitation adjacent and within pyrite crystals is consistent with the mode of

occurrence observed in basement lodes beneath the central anomaly. Thus at least a portion of the gold at the base of the sand is a placer deposit.

The anomalies in the transported regolith are more tightly constrained than corresponding gold distribution in the saprolite. Secondary gold within the saprolite is clearly distributed about basement lodes, but within the palaeochannel environment subsequent remobilization by groundwater has redistributed the placer gold within the underlying saprolite, providing a dual source for saprolitic gold enrichment.

6.0 CONCLUSION

Two separate lateritization events of differing intensity are recorded within the regolith of the Kalgoorlie region. The earlier event, which pre-dates palaeochannel incision was the more intense and resulted in an extensive well-developed laterite profile that is correlatable over the whole of the Yilgarn. The later event has occurred post-Late Eocene and has resulted in an extensive ferruginous upper profile and is best observed within the palaeochannel sediments where interference with the pre-existing profile does not occur.

Reconstructing pre-channel laterite profiles across the palaeochannels has resulted in a maximum depth of channel incision at Kurnalpi of 25-30 metres; Gindalbie 40 -50 metres; and the trunk channels 60 - 70 metres.

The pre-palaeochannel lateritization event probably occurred through the Mesozoic. It resulted in a laterite profile that was probably largely unmodified and extensive in the Kalgoorlie area. Palaeochannel incision has truncated the upper profile in the lowland areas, whereas post-Miocene colluvial action has resulted in extensive truncation in the upland areas.

Gold distribution at both study areas is mostly distributed about a vertical plane through the channel thalweg.

At Gindalbie gold distribution is secondary and is controlled by the chemistry of the mobilizing fluids and the depositional horizons. Gold patterns are basically horizontal - the result of deposition at the watertable. Virtually all gold is located within the reduced component of the palaeochannel sediments.

At Kurnalpi the palaeochannel flows over Archaean lode-style mineralization adjacent to the Avoca Shear. Gold distribution patterns within the palaeochannel sediments show a strong spatial association with known bedrock lodes; - with a modest downstream offset in the 10's of metres. Gold recovered from the base of the palaeochannel sand shows morphological evidence of placer deposition.

Secondary gold distribution patterns in the basement regolith display the dual influences of detrital gold at the base of the channel and lode-style mineralization along basement structures.

7.0 REFERENCES

Anand, R.R. and Smith, R.E. 1993. Regolith distribution, stratigraphy and evolution in the Yilgarn Craton - implications for exploration. *in*: An international conference on crustal evolution, metallogeny and exploration of the Eastern Goldfields. Australian Geological Survey Organisation, Extended Abstracts, Record 1993/54

Anand, R.R. Smith, R.E. & Butt, C.R.M. 1993. Definitions, Standardised Terminology and Classification of Regolith *In*: Exploration Geochemistry and Hydrothermal Geochemistry. Master of Economic Geology Course Work Manual 11, 2nd Ed. CODES, University of Tasmania.

Bird, M.I & Chivas, A.R. 1993. Geomorphic and palaeoclimatic implications of an Oxygen-isotope chronology for Australian deeply weathered profiles. *Australian Journal of Earth Sciences* **40** 345-358.

Butt, C.R.M. 1988. Genesis of Supergene Gold Deposits in the Lateritic Regolith of the Yilgarn Block. W.A. *in*: The Geology of Gold Deposits: The Perspective in 1988. Editors: R.R. Keays, W.R.H. Ramsay and D.I. Groves. *Economic Geology Monograph* **8**. Proceedings of Bicentennial Gold 88. 460-470.

Butt, C.R.M., Lintern, M.J., Robertson, I.D.M., & Gray, D.J., 1993. Geochemical exploration concepts and methods in the Eastern Goldfields Province *in*: An international conference on crustal evolution, metallogeny and exploration of the Eastern Goldfields. Australian Geological Survey Organisation, Extended Abstracts, Record 1993/54

Clarke, J.D.A. 1994a. Evolution of the Lefroy and Cowan palaeodrainages, Western Australia. *Australian Journal of Earth Sciences* **41**, 55-68.

Clarke, J.D.A. 1994b. Geomorphology of the Kambalda region, Western Australia. *Australian Journal of Earth Sciences* **41**, 229-239.

Commander, D.P., Kern A.M. and Smith, R.A. 1991. Hydrogeology of the Tertiary palaeochannels in the Kalgoorlie Region: Western Australia Geological Survey, Record 1991/10.

Davy, R. and El-Ansary, M., 1986. Geochemical patterns in the laterite profile at the Boddington gold deposit, Western Australia. *J. Geochem. Explor.*, **26**: 119-144

Kern, A.M. and Commander, P. 1993. Cainozoic stratigraphy in the Roe Palaeodrainage of the Kalgoorlie region, Western Australia. Geological Survey of Western Australia Professional Paper **34**.

Lawrance, L.M., 1990. Supergene gold mineralization. *in*: Ho S. E., Groves D. I. & Bennett J. M. (eds), Gold deposits of the Yilgarn Craton, Western Australia: Nature, Genesis and Exploration Guides. Geology Department (Key Centre) University Extension, The University of Western Australia. Publication **20**, 300 - 313.

Lawrance, L.M. 1993. Supergene mineralisation in the Eastern Goldfields Province, Western Australia. *in*: An international conference on crustal evolution, metallogeny and exploration of the Eastern Goldfields. Australian Geological Survey Oganization, Extended Abstracts, Record 1993/54

Lintern, M.J., 1994. Au and Ca concentration within pedogenic carbonate at the Gindalbie and Kurnalpi test sites. CSIRO memo to Mt. Kersey Mining N. L., unpublished

Mann, A.W. 1984. Mobility of gold and silver in lateritic weathering profiles: Some observations from Western Australia. *Economic Geology* **79**, 38-49.

Mann, A.W. and Webster, J.G., 1990. Gold in the exogenic environment, *in*: Geology of the Mineral Deposits of Australia and Papua New Guinea (Ed. F. E. Hughes). pp. 119-126. The Australasian Institute of Mining and Metallurgy

Ollier, C.D., Chan, R.A., Craig, M.A. & Gibson, D.L. 1988. Aspects of landscape history and regolith in the Kalgoorlie region, Western Australia. *BMR Journal of Australian Geology & Geophysics* **10**, 309-321.

Smith, R.E., Birrell, R.D. and Brigden, J.F., 1989. The implications to exploration of chalcophile corridors in the Archaean Yilgarn block. Western Australia, as revealed by laterite geochemistry. *J. Geochem. Explor.*, **32**: 169-84.

Smith, R.E. and Anand, R.R. 1990. Geochemical Exploration. *in*: Ho, S.E., Groves, D.I. and Bennett, J.M. (eds.) Gold Deposits of the Archean Yilgarn Block. Western Australia: Nature, Genesis and Exploration Guides, the University of Western Australia. Publication No. **20**, 331-336 pp.

Smyth, E.L. and Button, A. 1989. Gold exploration in the Tertiary palaeodrainage systems of Western Australia; Gold Forum on Technology and practices - World Gold '89, Reno, Nevada, No. 1989.

Swager, C.P. 1994. Geology of the Kurnalpi 1:100000 sheet. 1:100000 Geological Series - Explanatory Notes. Geological Survey of Western Australia

Swager, C.P., Griffin, T.J., Witt, W.K., Wyche, S., Ahmat, A.L., Hunter, W.M., McGoldrick, P.J. 1990. Geology of the Archaean Kalgoorlie Terrane - an explanatory note. Geological Survey of Western Australia. Record 1990/12

van de Graaff, W.J.E., Crowe, R.W.A., Bunting, J.A. and Jackson, M.J., 1977. Relict early Cainozoic drainages in arid Western Australia: *Zeitschrift fur Geomorphologie* N.F., v.**21**, p.379-400.

Wilson, A.F. 1984. Origin of quartz-free gold nuggets and supergene gold found in laterites and soils - a review and some new observations; *Australian Journal of Earth Sciences* **31**, 303-316

8.0 APPENDICES

Appendix 1. Anomalous drillhole intercepts from Gindalbie.

DRILLHOLE NO.	CO-ORDINATES	ANOMALOUS Au INTERSECTIONS	LITHOLOGICAL CONTROL ON MINERALIZATION
KSC 2155	10120E 14500N	2m @ 0.13 g/t from 30m	base of clay/top of sand interface
KSC 2132	10120E 14000N	2m @ 0.21 g/t from 32m	base of clay/top of sand interface
KSC 2133	10200E 14000N	6m @ 0.04 g/t from 22m	within reduced lacustrine clay unit
KSC 2134	10280E 14000N	2m @ 0.06 g/t from 24m	within reduced lacustrine clay unit
KSC 2142	10320E 14000N	4m @ 0.04 g/t from 28m	base of clay/top of sand interface
KSC 2128	10120E 13500N	6m @ 0.04 g/t from 26m	within reduced lacustrine clay unit
KSC 2127	10160E 13500N	2m @ 0.06 g/t from 32m	base of clay/top of sand interface
KSC 2115	10200E 13500N	4m @ 0.06 g/t from 28m	base of clay/top of sand interface
KSC 2117	10280E 13500N	4m @ 0.05 g/t from 26m	within reduced lacustrine clay unit
KSC 2118	10320E 13500N	4m @ 0.25 g/t from 28m	base of clay/top of sand interface
KSC 2119	10360E 13500N	4m @ 0.04 g/t from 28m	base of clay/top of sand interface
KSC 2120	10400E 13500N	6m @ 0.11 g/t from 26m	base of clay/top of sand interface
KSC 2121	10440E 13500N	2m @ 0.23 g/t from 26m	within reduced lacustrine clay unit
KSC 2126	10680E 13500N	2m @ 0.11 g/t from 18m	within reduced lacustrine clay unit
KSC 2097	10350E 12800N	2m @ 0.57 g/t from 28m	lacustrine clay/sandy clay interface
KSC 2095	10450E 12800N	6m @ 0.07 g/t from 20m	within reduced lacustrine clay unit
KSC 2094	10550E 12800N	2m @ 0.05 g/t from 28m	base of clay/top of sand interface
KSC 2093	10600E 12800N	4m @ 0.04 g/t from 28m	base of clay/top of sand interface
KSC 2092	10650E 12800N	4m @ 0.06 g/t from 26m	base of clay/top of sand interface
KSC 2091	10750E 12800N	4m @ 0.04 g/t from 30m	base of clay/top of sand interface
KSC 2099	10440E 12000N	4m @ 0.05 g/t from 22m	within reduced lacustrine clay unit
KSC 2100	10520E 12000N	2m @ 0.07 g/t from 32m	lacustrine clay/sandy clay interface
KSC 2101	10560E 12000N	2m @ 0.06 g/t from 30m	lacustrine clay/sandy clay interface
KSC 2102	10600E 12000N	4m @ 0.04 g/t from 28m	lacustrine clay/sandy clay interface
KSC 2104	10680E 12000N	4m @ 0.06 g/t from 30m	lacustrine clay/sandy clay interface
KSC 2105	10720E 12000N	6m @ 0.11 g/t from 32m	lacustrine clay/sandy clay interface
KSC 2106	10760E 12000N	4m @ 0.12 g/t from 30m	base of clay/top of sand interface
KSC 2107	10800E 12000N	6m @ 0.07 g/t from 20m	within reduced lacustrine clay unit
		6m @ 0.09 g/t from 28m	base of clay/top of sand interface
KSC 2110	10920E 12000N	2m @ 0.08 g/t from 32m	base of clay/top of sand interface
KSC 2111	10960E 12000N	6m @ 0.06 g/t from 42m	within sand unit
KSC 2112	11000E 12000N	2m @ 0.18 g/t from 42m	within sand unit
KSC 2075	10500E 11500N	2m @ 0.19 g/t from 70m	saprolite/saprock interface
KSC 2076	10600E 11500N	2m @ 0.19 g/t from 30m	base of clay/top of sand interface
KSC 2077	10700E 11500N	2m @ 0.12 g/t from 32m	base of clay/top of sand interface
KSC 2187	11000E 11500N	2m @ 0.16 g/t from 22m	below main redox front
KSC 2078	10520E 11000N	2m @ 0.39 g/t from 26m	channel clay/saprolite interface
		2m @ 0.06 g/t from 68m	saprolite/saprock interface
KSC 2080	10640E 11000N	3m @ 0.07 g/t from 72m	saprolite/saprock interface
KSC 2081	10680E 11000N	2m @ 0.12 g/t from 40m	within sand unit
KSC 2082	10720E 11000N	2m @ 0.42 g/t from 40m	within sand unit
KSC 2083	10760E 11000N	2m @ 1.00 g/t from 32m	base of clay/top of sand interface
KSC 2084	10800E 11000N	4m @ 0.11 g/t from 24m	within reduced lacustrine clay unit
KSC 2088	10960E 11000N	2m @ 0.05 g/t from 32m	base of clay/top of sand interface
KSC 2089	11000E 11000N	2m @ 0.50 g/t from 28m	lacustrine clay/sandy clay interface
		4m @ 0.13 g/t from 40m	base of sandy clay/top of sand interface
KSC 2090	11040E 11000N	2m @ 0.26 g/t from 44m	channel clay/saprolite interface
KSC 2020	10650E 10500N	2m @ 0.38 g/t from 28m	base of clay/top of sand interface
KSC 2021	10750E 10500N	2m @ 0.35 g/t from 32m	base of clay/top of sand interface
KSC 2022	10850E 10500N	2m @ 0.21 g/t from 48m	base of clay/top of sand interface
		8m @ 0.08 g/t from 52m	sand/saprolite unconformity
KSC 2026	11250E 10500N	4m @ 0.07 g/t from 58m	saprolite/saprock interface

Appendix 1. (cont.)

DRILLHOLE NO.	CO-ORDINATES	ANOMALOUS Au INTERSECTIONS	LITHOLOGICAL CONTROL ON MINERALIZATION
KSC 2177	9400E 10000N	6m @ 0.21 g/t from 26m	top of reduced clay
		2m @ 0.07 g/t from 58m	sand/saprolite unconformity
KSC 2178	9440E 10000N	6m @ 0.17 g/t from 26m	top of reduced clay
KSC 2176	9480E 10000N	2m @ 0.08 g/t from 16m	lower oxidized clay
		4m @ 0.13 g/t from 28m	within reduced lacustrine clay unit
KSC 2179	9520E 10000N	2m @ 0.10 g/t from 30m	within reduced lacustrine clay unit
		2m @ 0.08 g/t from 60m	sand/saprolite unconformity
KSC 2180	9560E 10000N	4m @ 0.14 g/t from 28m	within reduced lacustrine clay unit
		4m @ 0.15 g/t from 56m	sand/saprolite unconformity
KSC 2181	9600E 10000N	4m @ 0.09 g/t from 28m	within reduced lacustrine clay unit
		2m @ 1.82 g/t from 60m	sand/saprolite unconformity
KSC 2175	9640E 10000N	4m @ 0.08 g/t from 18m	lower oxidized clay
		4m @ 0.16 g/t from 28m	base of channel clay (no sand unit)
KSC 2173	9960E 10000N	2m @ 0.08 g/t from 42m	saprolite
KSC 2168	10240E 10000N	2m @ 0.25 g/t from 20m	immediately below main redox front
KSC 2165	10280E 10000N	2m @ 0.07 g/t from 22m	top of reduced clay
		4m @ 0.15 g/t from 38m	within sand unit
KSC 2169	10320E 10000N	1m @ 0.39 g/t from 81m	saprolite/saprock interface
KSC 2184	10360E 9750N	2m @ 0.07 g/t from 26m	base of clay/top of sand interface
		2m @ 0.18 g/t from 48m	kaolinitic sandy clay/sand interface
		2m @ 0.08 g/t from 72m	saprolite/saprock interface
KSC 2185	10520E 9750N	6m @ 0.10 g/t from 48m	upper saprolite

Appendix 2. Correlation co-efficients for multi-element analyses on spherical pisoliths from Gindalbie (see Table 3.4)

	Au	As	Mo	Sn	Sb	Ag	Pt	Pd	Pb	W	Bi	Cu	Zn	Be	Mn	Nb	U
Au	1																
As	-0.1972	1															
Mo	0.108651	0.491634	1														
Sn	-0.06871	-0.05643	-0.25165	1													
Sb	-0.59468	0.517847	0.112072	0.171895	1												
Ag	0.494407	-0.19853	0.112615	0.201218	-0.44112	1											
Pt	-0.04994	0.44838	0.193188	0.143894	0.562652	-0.18244	1										
Pd	-0.10049	0.713461	0.686101	-0.17993	0.38434	-0.07727	0.445116	1									
Pb	0.036786	0.555688	0.693549	-0.2475	0.153096	0.014088	0.006108	0.560222	1								
W	-0.0212	0.336552	0.367337	-0.01971	0.049583	0.301125	0.31052	0.445545	0.175026	1							
Bi	-0.15009	0.66939	0.473697	-0.05755	0.606233	-0.03541	0.777492	0.601043	0.37617	0.502502	1						
Cu	0.470821	-0.44162	0.685601	-0.0735	-0.50524	0.820565	-0.06704	0.333661	-0.19467	0.129568	-0.19066	1					
Zn	0.871632	-0.60017	0.342595	-0.03504	-0.53136	0.604384	0.05237	-0.19766	-0.30624	-0.12138	-0.13786	0.685575	1				
Be	0.859243	-0.52776	0.441791	0.029818	-0.46269	0.657675	0.064452	-0.22445	-0.14084	-0.12269	-0.1162	0.675877	0.972523	1			
Mn	0.856454	-0.62293	0.350359	-0.05339	-0.52008	0.631589	0.085927	-0.20292	-0.34522	-0.0974	-0.08251	0.687551	0.994647	0.961608	1		
Nb	0.575475	-0.24058	0.53077	-0.14976	-0.3162	0.663486	-0.0992	0.116766	-0.02492	0.355177	-0.10167	0.69857	0.788091	0.789752	0.780228	1	
U	0.551816	-0.2572	0.370882	0.213053	-0.24073	0.69327	-0.05112	-0.23793	0.337744	-0.18347	-0.05398	0.517842	0.736858	0.783097	0.723384	0.727797	1